HEAT TRANSFER AND DENSITY DISTRIBUTION MEASUREMENTS BETWEEN PARALLEL PLATES IN THE TRANSITION REGIME

by

WILLIAM P. TEAGAN

B.Sc. Brown University
(1961)

M.Sc. Massachusetts Institute of Technology
(1963)

SUBMITTED IN PARTIAL FULFILLMENT OF THE

REQUIREMENTS FOR THE DEGREE OF

DOCTOR OF PHILOSOPHY

at the

MASSACHUSETTS INSTITUTE OF TECHNOLOGY

MAY 1967

Signature of Author.....
Department of Mechanical Engineering, May 15, 1967

Certified By.....
Thesis Supervisor

Accepted By.....
Chairman, Departmental Committee on Graduate Students

HEAT TRANSFER AND DENSITY DISTRIBUTION MEASUREMENTS BETWEEN PARALLEL PLATES IN THE TRANSITION REGIME

by

WILLIAM P. TEAGAN

Submitted to the Department of Mechanical Engineering on May 15, 1967, in partial fulfillment of the requirements for the degree of Doctor of Philosophy.

ABSTRACT

The heat transfer and density distribution were experimentally determined for a rarified gas at rest between two flat plates. Both argon and nitrogen were used as test gases. Particular attention was focused on obtaining measurements in the transition regime where the ratio of plate spacing to mean free path was between 1 and 20. The accommodation coefficients of the gas-surface combinations used were determined from heat transfer measurements made in the free molecule regime. The gas density distribution was measured by observing the luminescence produced by an energetic electron beam traversed between the plates.

The experimental results for argon were compared directly with the analytical results of Wang-Chang and Uhlenbeck, Gross and Ziering, and Lees. The average agreement between the heat transfer measurements and the four-moment analytical results is within 2 percent and for the density ratio profiles within 3 percent.

Thesis Supervisor: George S. Springer
Title: Assistant Professor of Mechanical Engineering

ACKNOWLEDGEMENT

The author acknowledges the encouragement and advice provided by his thesis supervisor, Professor George S. Springer, and by Professors Ain N. Sonin and Paul B. Scott who served on his committee. In addition, the author wishes to thank the Fluid Mechanics Laboratory technical staff for their invaluable help in the construction of the experimental apparatus.

This research has been sponsored by the Advanced Research Projects Agency (Ballistic Missile Defense Office) and technically administered by the Fluid Dynamics Branch of the Office of Naval Research under Contract Nonr-1841(93). The work was done in part at the Computation Center at the Massachusetts Institute of Technology.

TABLE OF CONTENTS

LIST OF FIGURES

I. INTRODUCTION

The observed variation of heat transfer with pressure has the form indicated in Figure 1.1. This plot indicates that the curve can be divided into three regions, these being: the continuum, transition and free molecule regimes. The continuum limit is characterized by a Knudsen number which is small compared to one ($KN = \lambda/D << 1$), where D is a characteristic geometric length and λ the mean free path of molecules in the gas. In such a case, the vast majority of collisions experienced by a molecule are with other molecules and molecule-boundary collisions are relatively rare. The free molecule limit is characterized by a large Knudsen number ($\lambda/D >> 1$). In such a gas, intermolecular collisions are relatively rare and, therefore, the majority of collisions experienced by a molecule are with the boundaries.

Both these limits can be described analytically because of the simplifying assumptions afforded by being able to say that the process is controlled respectively by intermolecular collisions (continuum) or molecule-boundary collisions (free molecule). The continuum heat conduction is described by the well known Fourier relation, i.e., the heat transfer is proportional to the temperature gradient. The free molecule heat conduction is given by the Knudsen expression[19] which indicates that the heat conduction is linearly proportional to pressure.

The description of the heat conduction and the density profiles in the transition regime is complicated by the fact that the simplifying

assumptions which allowed for the analytical descriptions of the continuum and free molecule limits are no longer valid. Recently, however, the revived interest in rarified gas problems has resulted in several investigators[1-8] addressing themselved to the problem of analytically describing on a microscopic level the state of the gas in the transition regime. Many of these investigators focused their attention on the parallel plane geometry shown in Figure 1.2. These analytical results describe the heat transfer and the distribution of density and temperature between the plates as a function of Knudsen number. Although the various analytical results are in basic agreement among themselves in the continuum and free molecule limits, in the transition regime they can differ by 25 percent for the heat transfer and 30 percent for the density distribution.

There is a lack of reliable experimental measurements with which to compare the results of these analyses. Dybbs and Springer[19] measured the heat transfer in the transition regime for the case of a cylindrical geometry and, therefore, their results cannot serve as a test for the plane layer geometry under consideration. Lazareff[17] and Mundell and West[18] utilized a plane layer geometry in order to measure temperature profiles in rarified gases by means of thermocouples. Both investigations succeeded in experimentally varifying the temperature discontinuity between the plate temperature and that of the gas adjacent to it which was predicted to occur by Smoluchowski.[9] In these investigations the radiation and support losses were not taken into account. Also, the temperature jump effects between the thermocouples and the adjacent gas were not considered. It is, therefore,

difficult to relate the temperature of the thermocouples to that of the adjacent gas. In addition, no heat transfer measurements between the plates were made and, therefore, the accommodation coefficients for the gas-surface combinations utilized were not determined. Bienkowski[8] measured the heat transfer as a function of pressure between gold plated flat plates using helium as a test gas. Comparison of his results with those of Lees[4] indicates general agreement on the transition regime. The extent of this agreement is, however, difficult to ascertain since the author does not discuss the expected accuracy of his measurements or the degree of agreement between his measurements and theory.

Thus, it is evident that little experimental data regarding the heat transfer and the density distribution for a gas in the transition regime is available. However, the parallel plate geometry has often been used as a test case for the various analytical models whose purpose it is to describe the transition range heat transfer and density distribution.

The purpose of this investigation was to perform an experiment which could indicate the relative accuracy of the various analyses which are applicable for the case of a parallel plate geometry. To accomplish this, both the heat transfer and the density distribution between parallel plates were measured in the transition regime.

Heat transfer measurements were also made in the free molecule regime so that an average value of the accommodation coefficient could be determined for the various gas-surface combinations utilized.

The density distribution measurements were made by measuring the luminescence produced by the passage of an energetic electron beam through the test gases. This method was first utilized by Schumacker and Gadomer[25] and has been recently used by several investigators[24-28] to measure density distributions in rarified gas flows.

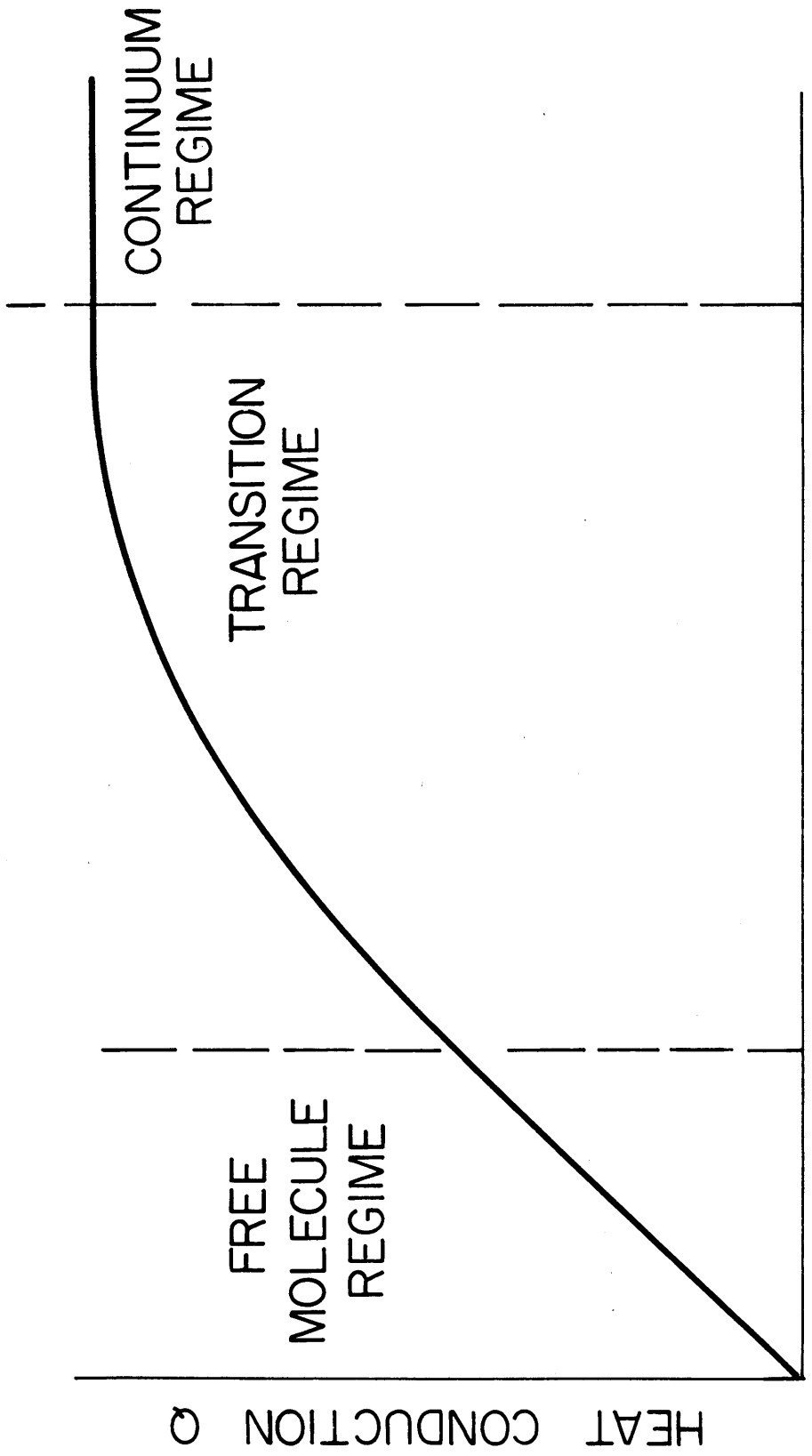

Fig. 1.1 Variation of Heat Transfer with Pressure

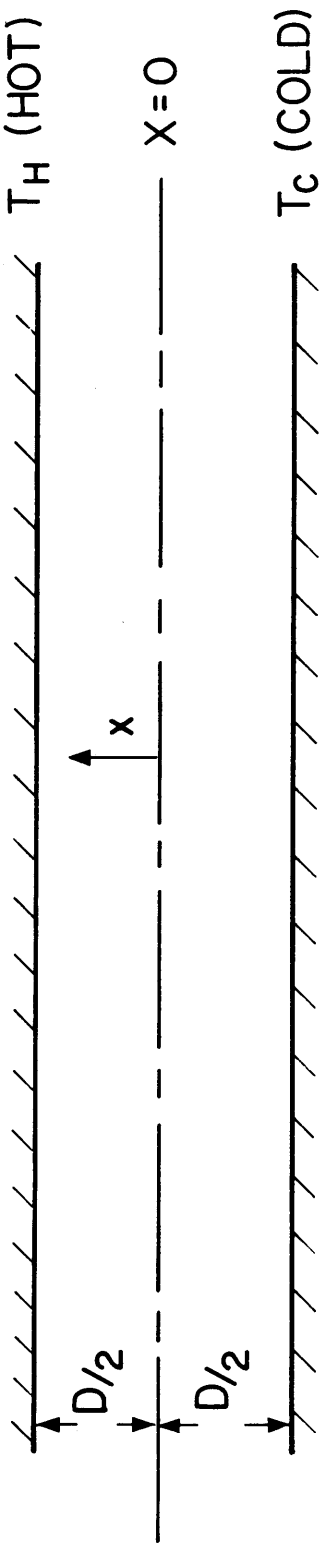

Fig. 1.2 Parallel Flat Plate Geometry

II. DISCUSSION OF THE ANALYSES

The analyses with which the experimental measurements are compared are discussed in this section. Particular attention is focused on the physical assumptions regarding geometry, molecular model, temperature differences, and boundary conditions utilized in the various analyses. By doing this it is possible to judge to what extent the conditions of the experiment were consistent with these assumptions. Also, it was desirable to measure those values of the relevant parameters which could best indicate the accuracy of the various analytical approaches. The analyses of Wang-Chang and Uhlenbeck,[1] Gross and Ziering,[2,3] Lees,[4] Lavin and Haviland,[5,6] and Frankowski[7] are compared with experimental measurements.

Several of the terms used in these descriptions are first explained.

In all of the analyses the boundary conditions are characterized by an accommodation coefficient, ε. If full accommodation is assumed ($\varepsilon = 1$), then, upon collision with a boundary, the rebounding molecules are considered to have a Maxwellian distribution characteristic of the surface temperature. The assumption of incomplete accommodation ($\varepsilon \neq 1$) implies that a fraction ε, of the incoming molecules leave the wall with a Maxwellian distribution characteristic of the wall temperature and the fraction $(1 - \varepsilon)$ experience specular reflection at the wall.

The basic assumption of the "linearized" analysis is that the temperature difference between the plates is sufficiently small so that; $\frac{\Delta T}{T_o} << 1$. With this assumption the distribution function can be expressed as:

$$f(\bar{v},x) = f_m(T_o)[1 + \phi(\bar{v},x)]$$

where $f_m(T_o)$ is a Maxwellian distribution characteristic of the plate centerplane conditions and $(\phi(v,x))$ is a small disturbance quantity which differs in form for each analysis. The problem is then described by the linearized Boltzman equation in terms of $(\phi(v,x))$.

Wang-Chang and Uhlenbeck:[1]

The Wang-Chang and Uhlenbeck analysis allows for arbitrary values of the accommodation coefficient, ε. The disturbance, $(\phi(v,x))$, is expanded in terms of the eigenfunctions of the Boltzman collision operator. The solution is carried out for a gas of Maxwell molecules.

Results are obtained for three successive approximations. No further approximations are attempted because the calculations become very involved and, also, the first three calculations do not numerically differ significantly from one another for such quantities as the heat transfer.

Both the second and third approximations indicate "molecular boundary layer" effects which show up mathematically in the appearance of hyperbolic sines and cosines. The deviation from a linear density profile due to the "molecular boundary layer" effect is very small (1%)

for the second approximation, but becomes more pronounced for the third approximation.

The second approximation results are in a form which is easy to use for all accommodation coefficients. Unfortunately, the third approximation is in a very cumbersome mathematical form, and therefore, is not used for direct comparison with experimental data.

Frankowski et al:

This analysis is carried out only for the case of full accommodation. Similarly to Wang-Chang and Uhlenback, the solution for the disturbance, ϕ, is expressed as an expansion in terms of the eigenfunctions of the Boltzman collision operator. Results are obtained for a gas of hard sphere molecules.

The solutions were all obtained by means of a computer and are, therefore, only in numerical form. The numerical results presented for the temperature distribution indicate the "molecular boundary layer" effect. The departure from a linear profile is quite small being a maximum at values of D/λ of about 10 where the departure is about 4 percent.

No results are presented for the heat transfer.

Gross and Ziering:

The Gross and Ziering analysis allows for arbitrary values of the accommodation coefficient.

The small distrubance, $(\phi(\bar{v},x))$, is approximated by a half range polynomial in velocity space in terms of initially unknown spatial functions. These spatial functions are determined by taking half range velocity moments of the Boltzman equation. The moments chosen are those corresponding to m, mv_x, $\frac{mv^2}{2}$, and $\frac{mv_x v^2}{2}$. Each of these moments yields two equations, one for integrations over all positive x velocities, the other for integrations over all negative x velocities.

The sum of any pair of half range moment equations is a full range moment equation. The first three of these sums correspond to the collisional invariants of mass, momentum, and energy and, therefore, the collision term for those sums is zero. The sum for the fourth pair of half range moment equations does not correspond to any conservation law.

For the eight-moment method all four pairs of moment equations are utilized and the linearized, half range, collision integrals evaluated in terms of the unknown spatial functions for both hard sphere and Maxwellian molecules.

For the four-moment method each pair of equations is summed to yield four full range moment equations. This gives the full range moment equations corresponding to the three collision invariants and the full range moment equation pertaining to the transport of energy, i.e. $C_x m \frac{v^2}{2}$.

The results for the eight-moment analysis indicate some of the peculiar features of rarified gas flows, such as:

(1) A pressure variation in the vicinity of the plates as a result of the "velocity skewness" introduced by the

boundary. The actual deviation from a constant pressure is very small numerically but is important from a fundamental point of view.

(2) A "molecular boundary layer" effect within a few mean paths of the plates which shows up by the temperature and density profiles deviating from being purely linear near the plates. As seen in Figure 2.2 this departure from a linear profile can be rather significant for the eight-moment method.

The four-moment results are not sufficiently sensitive to indicate the pressure variation and the "molecular boundary layer" effects. The temperature and density profiles indicated by the four-moment results are, therefore, linear.

Lees:

The physical assumptions used in the Lees approach are not as strict as those used in the linear analysis. The non-linear Lees method makes no assumption that $\frac{\Delta T}{T} << 1$, and, therefore, should apply for large as well as small temperature differences. The non-linear results are obtained for a value of the accommodation coefficient of unity, but the linearized results are extended (appendix 1) to include the case of arbitrary values of the accommodation coefficient.

Lees assumes a special form of the distribution function which he calls the "two sided Maxwellian" which is:

$$f^{\pm} = \frac{n^{\pm}(x)}{[2\pi kT^{\pm}(x)]^{3/2}} \quad \mathrm{Exp}\{\frac{-mv^2}{2kT^{\pm}(x)}\}$$

This form of the distribution function has the "two sides" character essential for describing highly rarified gas flows and can also provide for a smooth transition from rarified flows to the Navier-Stokes regime. The four spatial functions $n^{\pm}(x)$ and $T^{\pm}(x)$ are initially undetermined functions of x. These four functions are determined by making use of the four full range moments of the Boltzman equation corresponding to m, mv_x, $m\frac{v^2}{2}$ and $mv_x\frac{v^2}{2}$. The first three moments correspond to the collisional invariants and, therefore, the collision integral appearing on the right side of the Boltzman equation is zero for these moments. The fourth moment corresponds to the heat flux. The collision integral involved in this moment, which does not correspond to a collisional invariant, is evaluated for the case of Maxwellian molecules. It is seen then that the four moments of the Boltzman equation used by Lees are those used by Gross, Ziering in their four moment, full range, results.

The final results obtained in this non-linear analysis indicate that:

(1) The pressure between the plates is constant

(2) No molecular boundary layer effects

(3) The temperature distribution is NOT symetric about the plate centerplane as is indicated by the linear analysis. This lack of symmetry is what one would expect for large temperature differences. The non-linear results indicate that the temperature slip at the cold wall, where the density is highest, is smaller than at the hot wall where the density is smallest.

The linearized results indicate a constant pressure distribution and indicate a linear profile for the density distribution just as does the four moment method of Gross, Ziering.

Lavin and Haviland:

This analysis utilizes the basic Lees approach and the results are applicable for arbitrary values of $\frac{\Delta T}{T}$ (i.e. non-linear) and only for full accommodation. Two solutions are presented, the first a four-moment solution for hard sphere molecules, the second a six-moment solution for Maxwellian molecules.

The most general form assumed for the trial distribution function is:

$$f^{\pm} = \frac{2n^{\pm}(x)}{\pi^{3/2} C_x^{\pm}(x) C_y^{\pm}(x)} \; \mathrm{Exp}\left[-\left(\frac{u_x^2}{C_x^{\pm}(x)} + \frac{u_y^2 + u_z^2}{C_y^{\pm}(x)^2}\right)\right]$$

This form of the distribution function is different from that of Lees only in that it allows for the division of each velocity component by a different function.

Four Moment Solution:

The general expression for the distribution function is specialized to a four function distribution by letting $C_x^{\pm} = C_y^{\pm} = C^{\pm}$. The four unknown spatial functions $n^{\pm}(x)$ and $C^{\pm}(x)$ are determined by taking the same four, full range, moments of the Boltzman equation utilized by Lees.

The results are very similar to those of Lees for both the heat transfer and temperature distribution. Similarly to all the other four

moment methods, the results do not exhibit a pressure variation between the plates.

Six Moment Solution:

For the six-moment solution, all six spatial parameters are used in the distribution function. The three moment equations used in addition to those corresponding to the collisional invariants are those corresponding to mv_x^2, mv_x^3, and $mv_x v_y^2$. To facilitate the evaluation of the collision terms associated with these moments, the analysis is performed for Maxwellian molecules.

The results for the six-moment method are very similar to those of the Lees four-moment analysis, the most significant difference being that the six-moment method indicates a small variation of pressure between the plates.

Discussion:

Some numerical results obtained from the various analyses described are shown in Figures 2.1 and 2.2. These results are all shown for the case of full accommodation.

It is seen that the results for the heat transfer ratio Q/Q_{fm}, divide into two groups:

(1) The four-moment methods both linear and non-linear, in which are also included the Wang-Chang and Uhlenbeck results.

(2) The eight-moment methods of Gross and Ziering.

In Figure 2.1, the four-moment, non-linear, results of Lavin and Haviland are shown. Their six-moment results and the Lees non-linear results are not shown since they fall very close to these for small temperature ratios.

The disagreement between these two groups is about 15 percent in the important range corresponding to D/λ values from 1 to 10. The four-moment and the Wang-Chang and Uhlenbeck results, on the other hand, agree rather closely (5 percent) with one another, in this transition regime.

Two plots for the density distribution profiles are shown in Figure 2.2, one for $D/\lambda = 5$ and the other for $D/\lambda = 1$. The plot for $D/\lambda = 5$ indicates that the density profiles are not clearly separated into two groups as with the heat transfer results. For $D/\lambda = 1$, however, the separation of the profiles into two distinct groupings is very pronounced with the average difference between them being about 30 percent. For all values of D/λ the available Frankowski results indicate close agreement with the Gross and Ziering eight-moment results for the density distribution profiles.

As seen in Figures 5.4 and 6.1, which compare the measured heat transfer ratios and density profiles with the results of analysis, the disagreement between the eight-moment results and the four-moment results become even more pronounced for non-unity values of the accommodation coefficient than for the full accommodation case. The agreement between the four-moment results is, however, still evident.

Although it might be reasonable to expect that some of these solutions are quite accurate over the full range of conditions, some degree of uncertainty exists as to which solutions are most valid. The disagreement between the various analytical results in the transition regime is sufficiently large so that an accurate experiment designed to measure the heat transfer and the density distribution between unequally heated flat plates should indicate the relative accuracy of the various approaches.

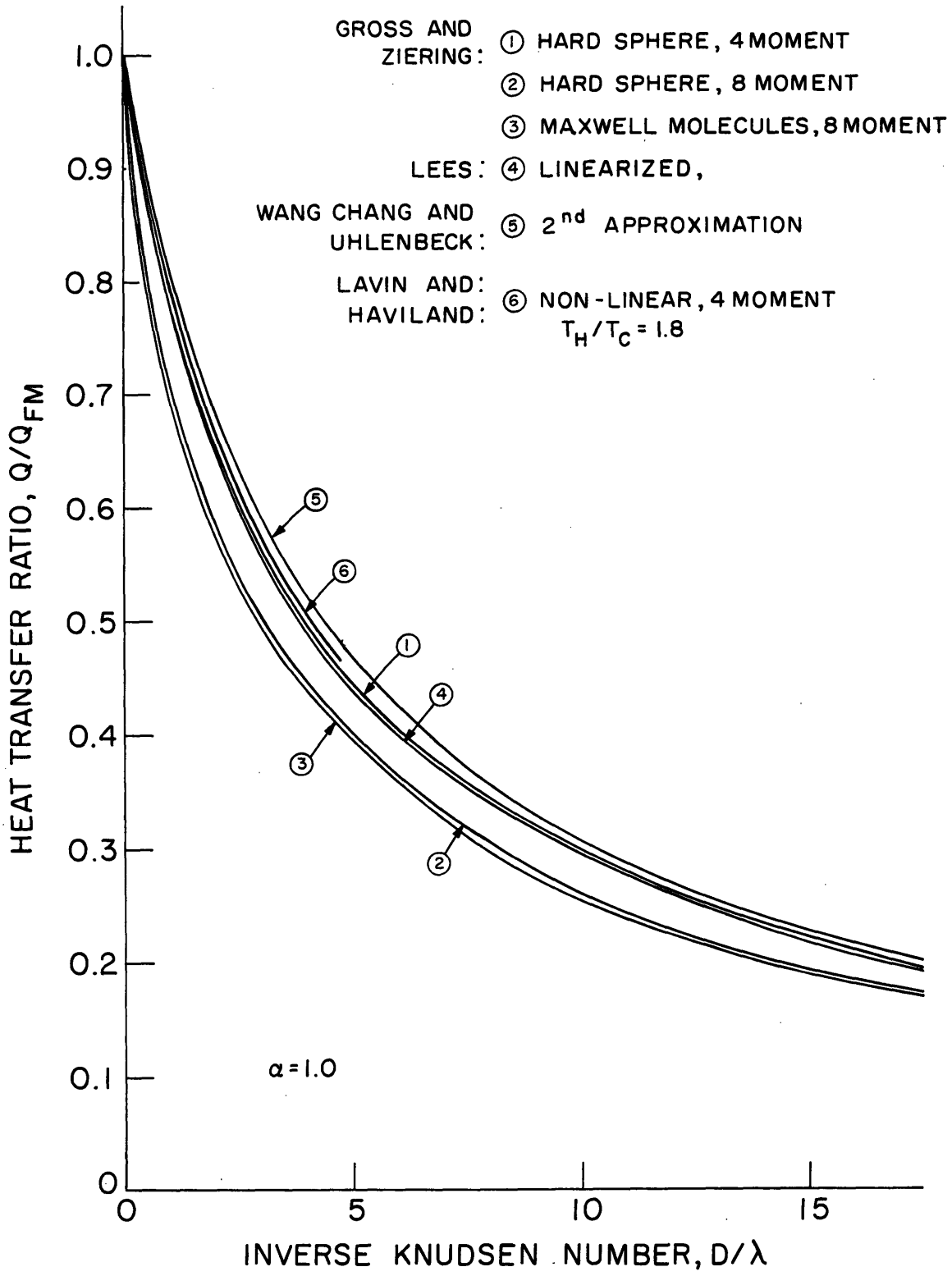

Fig. 2.1 Comparison of the Analytical Heat Transfer Results For the Case of Unity Accommodation

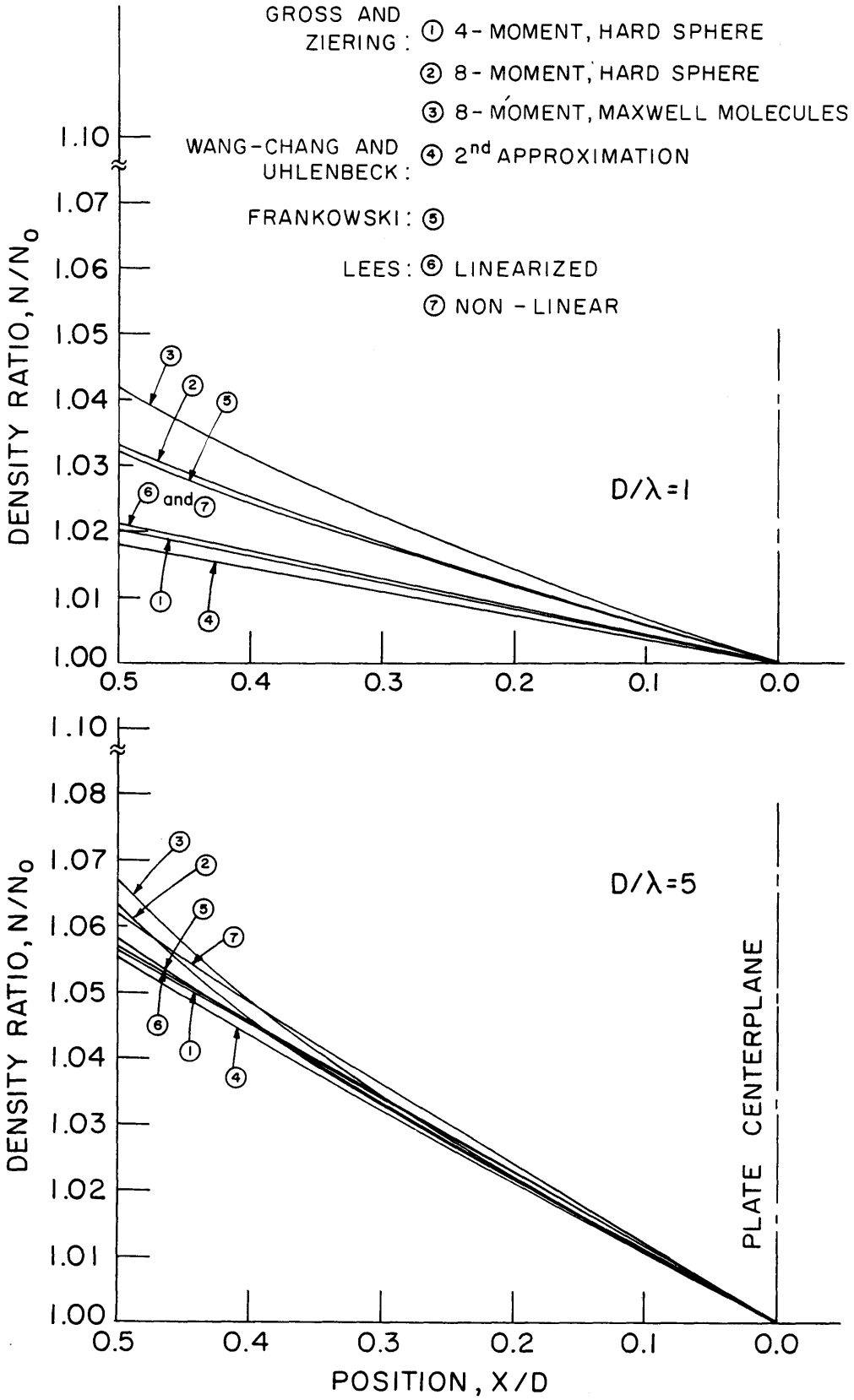

Fig. 2.2 Comparison of the Analytical Density Distribution Results for the Case of Unity Accommodation

III. EXPERIMENTAL APPARATUS

In order to obtain measurements of the heat transfer and the density distribution between parallel plates and be able to compare these measurements with the results of analyses, the following experiment was performed:

First, the heat transfer between the plates was measured for the complete range of D/λ values from free molecule to continuum conditions. From the free molecule heat conduction measurements a value of the accommodation coefficient was obtained. This value of the accommodation coefficient was used in evaluating values for the heat conduction and density distribution from the analytical results.

To obtain the density distribution profile, a narrow, energetic electron beam was sent between the plates and the luminescence from a given portion of the beam measured by a photomultiplier tube. By arranging it so the position of the beam could traverse the spacing between the plates, it was possible to obtain the density ratio, $N(x)/N_o$, by forming the ratio of photomultiplier tube readings.

The experimental apparatus used to perform this experiment consisted essentially of four separate systems:

(1) A vacuum system designed for use with an electron beam probe.

(2) A flat plate assembly which was used to measure the heat transfer between parallel flat plates under vacuum conditions and, also, was used for the density distribution measurements.

(3) An electron beam generator along with a shielded cup which collected the beam current.

(4) An optical-photomultiplying tube system which measured the luminescence from a desired section of the beam.

Each of these components of the experimental apparatus is discussed individually in the following sections.

3.A. The Vacuum System

The vacuum system had to be designed such that the test chamber and the electron gun chamber could be operated with a substantial pressure differential during density distribution measurements. A sketch of the principal components of the vacuum system is shown in Figure 3.1. The reasons a pressure differential between the two chambers had to be maintained are:

(1) The electron gun could not be operated at pressure above $(5)10^{-4}$Torr.

(2) The test gas pressure had to be varied from between $(3)10^{-3}$ to $(40)10^{-3}$Torr during density distribution measurements.

To accomplish this pressure differential it was necessary that during density distribution measurements the main connection between the test section and the pumping system be closed (valve A). Under these conditions the only connection between the electron gun chamber and the test chamber was through the 1 mm. hole through which the

electron beam entered the test chamber. The 1 mm. hole was sufficiently small so that the pressure of the gas in the test section could be brought up to at least 50 x 10^{-3} Torr. while still maintaining a sufficiently low vacuum in the electron gun chamber.

The main components of the vacuum system are described below:

The test section was a stainless steel "well" 45 cm. diameter and 19 cm. deep. On top of the well was placed a 45 cm diameter 32 cm. high bell jar which sat on a smoothly machined surface. The bottom of the well was provided with ten 1 in. holes for the feed throughs necessary for the instrumentation of the experiment. On one side of the well a 6.35 cm. diameter window was provided for observation of the electron beam with the optical system. The main means for evacuating the test section was through a 5.1 cm. inner diameter tube which could be closed by a valve (valve A) during density distribution measurements. The ultimate vacuum in the test section with the valve open was about 10^{-6}Torr. With the valve closed the ultimate vacuum achieved by pumping through the 1 mm. hole was (5)10^{-5}Torr. Pressures in the test section were read with a high precision McLeod gage. The test gas entered the test section through a leak valve which allowed a fine control of the pressure.

The electron gun chamber was a stainless steel cylinder 28 cm. long and 10 cm. in diameter. The back of the chamber was provided with a flange on which the electron gun base plate could be mounted. The top of the chamber was provided with a 6.35 cm. diameter window for observing the gun during operation. The connection to the pumping system was by a

13.3 cm. diameter section of stainless steel pipe which was cooled by a water coil. A baffle was provided to minimize the oil migration to the electron gun chamber. Pressures in the gun chamber were read by means of an ionization gage.

The system was evacuated by a CVC 4 inch oil diffusion pump (Model PMC-4B) connected to a Welch model 1402 Duo Seal mechanical pump. Corning 704 diffusion pump oil was used in the diffusion pump.

3.B. Flat Plate Apparatus:

The flat plate system used for measuring heat conduction through gases is shown schematically in Figure 3.2. The plate assembly consists of an electrically-heated plate, referred to as the hot plate, sandwiched between two water-cooledplates (cold plates). The main advantage of this arrangement is that it is considerably simpler than those requiring elaborate compensating heaters for minimizing heat losses from the hot plate. The three plates were separated from each other and held parallel for any given spacing by two sets of eight Plexiglas spacers each having a cross-sectional area of 0.0252 cm^2. The entire plate assembly was kept horizontal during the experiments.

Two sets of plate systems were constructed, one of aluminum and one of copper in order to test the effect of the material used on the results. Except for the materials used the two systems were identical. The cold plates were 25.4 cm. dia. and 1.27 cm. thick. Soldered to one side of these plates were 0.635 cm. id and 0.476 cm. od aluminum (copper) tubes arranged in coils as shown in Figure 3.2. The plates were cooled

by water flowing through the coils. The coils were connected to the water supply with Tygon tubing. Water was supplied to the tubes directly from the main, as it was found that its temperature was sufficiently constant during the period of any given experiment.

The hot plate assembly consisted of a heating element placed between two 25.4 cm. dia. and 0.238 cm. thick aluminum (copper) plates. The heating element was made by arranging No. 30 Chromel high resistance wire in a zig-zag pattern between two bondable Teflon sheets. The resistance wire was attached to one of these sheets with epoxy. The thickness of the heating element thus formed was about 0.0396 cm. The two hot plates were separated by eight 0.0794 cm. thick aluminum (copper) spacers (see Fig. 3.2) and then riveted together by eight 0.159 cm. dia. rivets. The total thickness of the hot plate was 0.555 cm. The purpose of this small thickness was to reduce heat losses from the edges. Power to the heater was supplied from the main electric line and was controlled with an ac transformer. The power input to the plate was determined by measuring with a vacuum tube voltmeter the potential drop across the wires leading directly into the heating element and the potential drop across a standard one-ohm resistance placed in series in the circuit.

The temperatures of the cold and hot plates were monitored with ten chromel-alumel thermocouples placed at the bottoms of 0.1587 cm. dia. "wells" ending about 0.04 cm. from the surface of the plates. The thermocouples were arranged and connected as shown in Fig. 3.3, permitting the simultaneous measurements of the temperatures at the centers of the plates,

the temperature difference between the hot and cold plates and the temperature drop along each plate. The temperature drops along the cold plates (connections 5-5 and 6-6, Fig. 3.3) were always less than 0.05°C. The temperature drops along the hot plates (connections 7-7 and 8-8) were generally below 0.1°C except near atmospheric pressures where they sometimes reached 0.5°C. In the reduction of the data these changes in temperature were neglected and the temperatures at the centerline (points 1-4, Fig. 3.3) were taken to be the plate temperatures.

The flat plate assembly was mounted on a plexiglas frame which made it possible to perform the following tasks while still under vacuum:

(1) After the heat transfer measurements were completed, it was possible to lower the bottom cold plate from the upper hot-cold plate assembly so that the density distribution data could be taken. The distance between the hot plate and the lower cold plate could be varied from 1.9 cm. to 2.9 cm.

(2) So that the position of the electron beam relative to the plates could be continuously varied, it was possible to move the entire plate assembly up and down in a vertical direction a total vertical distance of 3.2 cm.

A sketch of the plate system and this frame is shown in Figure 3.4

The vertical position of the plates relative to a base position could be determined by either an ordinary scale with a pointer or by a micrometer. The position of the beam for the final data readings

was determined by the micrometer.

The lower cold plate was lowered to its final position for making density distribution curves by mechanically pulling out three stops which held it in its upper position. The stops were pulled out by lowering the plates so that the bottom of the stop mechanisms came in contact with point A. Further lowering of the plates caused the stops to be pulled out by lever action as can be seen in Figure 3.4

The place assembly was raised and lowered by means of a screw mechanism which is also shown in Figure 3.4.

3.C. The Electron Beam System:

The electron beam system consisted of an electron gun capable of producing a narrow, high eneegy, electron beam and a collection cup which measured the electron beam current. A set of deflection plates were provided for aligning the beam parallel to the plates. A sketch of this system is shown in Figure 3.5. Both of these components along with their supporting equipment are described below:

The electron gun was the type commonly used in television tubes and is sketched along with some typical operating voltages in Figure 3.6. For purposes of this experiment the commercial oxide coated cathode which came with the gun was removed and a tungsten filament .005 in. in diameter was used as the electron source. The tungsten filament was used in order to avoid the problems that have been observed when using commercial cathodes.[24] These problems include poor performance after exposure to atmospheric pressure and sensitivity

to vacuum pump oil. The tungsten filament was powered by a variac controlled filament transformer which was insulated for 12 KV. The voltages for the accelerating and focusing plates were supplied by a regulated Sorenson high voltage supply (model 5030-4) and a Potter high voltage power supply.

The electron gun assembly was mounted on a base plate which was provided with the necessary high voltage feed throughs.

The electron beam was collected in a cup which is shown in Figure 3.5. The cup consisted of a cubical stainless steel inner chamber about 2.5 cm. on a side which was maintained at 67 volts. The inner chamber was insulated by a 0.3 cm. layer of teflon. Finally, there was an outer stainless steel shielding cup which was maintained at ground potential. A 1.2 mm. diameter hole was provided so that the electron beam could enter the inner chamber. The cup was designed in this way so that only the electrons in the beam were actually collected and measured. It was found that if the collection cup was not shileded that the current measured was a function of pressure for constant electron gun conditions. This was probably because an exposed cup can also collect many of the secondary electrons present in the gas.

The electron beam current was measured with a DC Vacuum Tube Voltmeter.

In order to adjust the beam position so that the beam entered the hole in the collection cup, a set of electrostatic deflection plates was provided. The deflection plates were mounted in the test chamber

right after the hole connecting the electron gum chamber to the test chamber. The plate voltages were supplied by two Lambda model C-261M regulated voltage supplies.

3.D. The Optical System

The optical system is shown schematically in Figure 3.7. It consisted of the lens system of a Praktine FX camera which focused an image of the luminescent beam on an adjustable slit placed in the focal plane of the camera (i.e. the plane usually occupied by the film). Directly behind the slit there was a model 6655A RCA photomultiplying tube. The output of the photomultiplying tube was measured on a Kiethly model 610B electrometer.

The length of the slit was such that the luminescence from a 1 cm. length of beam was measured. The slit width (1.0 mm) was sufficiently large to measure the total luminescence from this beam length and not just a portion of the centrol core.

The housing for the photomultiplying tube was cooled by an ice water bath which reduced the noise level to a negligible level for the operating conditions used.

The Praktina FX camera is the type where one can observe on an etched glass (see Fig.3.7) what is being focused on the camera focal plane by having mirror "C" in the down position. For purposes of this experiment the etched glass was replaced by a piece of plexiglass on which there was inscribed a horizontal line. This line and the adjustable slit were placed so that, if the beam was focused on the line with

the mirror in the "down" position, it would be focused on the slit with the mirror in the "up" position. This made it possible to be able to accurately align the beam image with the slit. That this arrangement worked correctly was indicated by the fact that the photomultiplying tube output was a maximum under these conditions.

The entire optical-photomultiplying tube system was placed on a platform which could be moved very accurately in the vertical direction by a screw mechanism. This was done so that the beam image could be lined up with the slit.

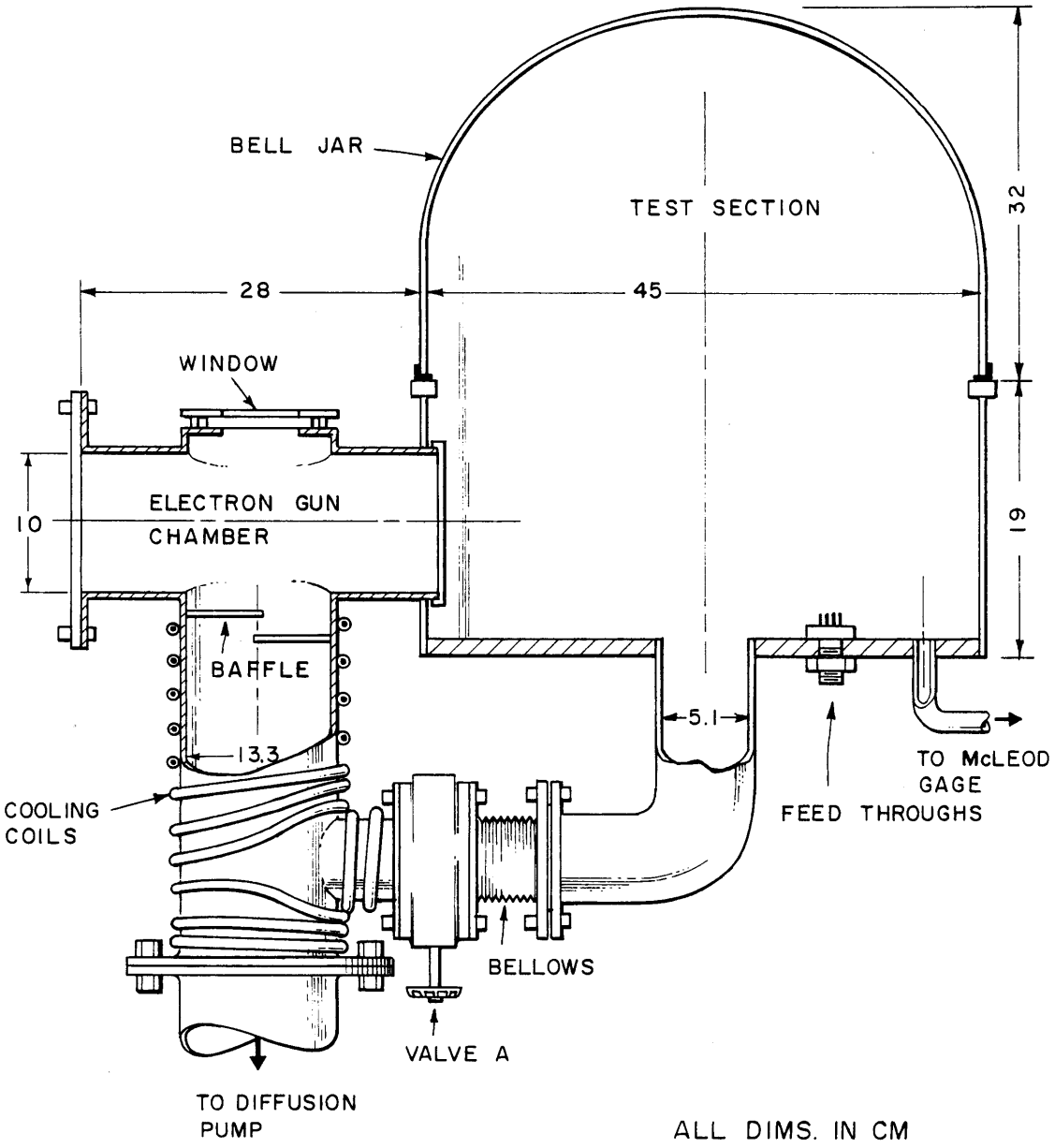

Fig. 3.1 Schematic of the Vacuum System

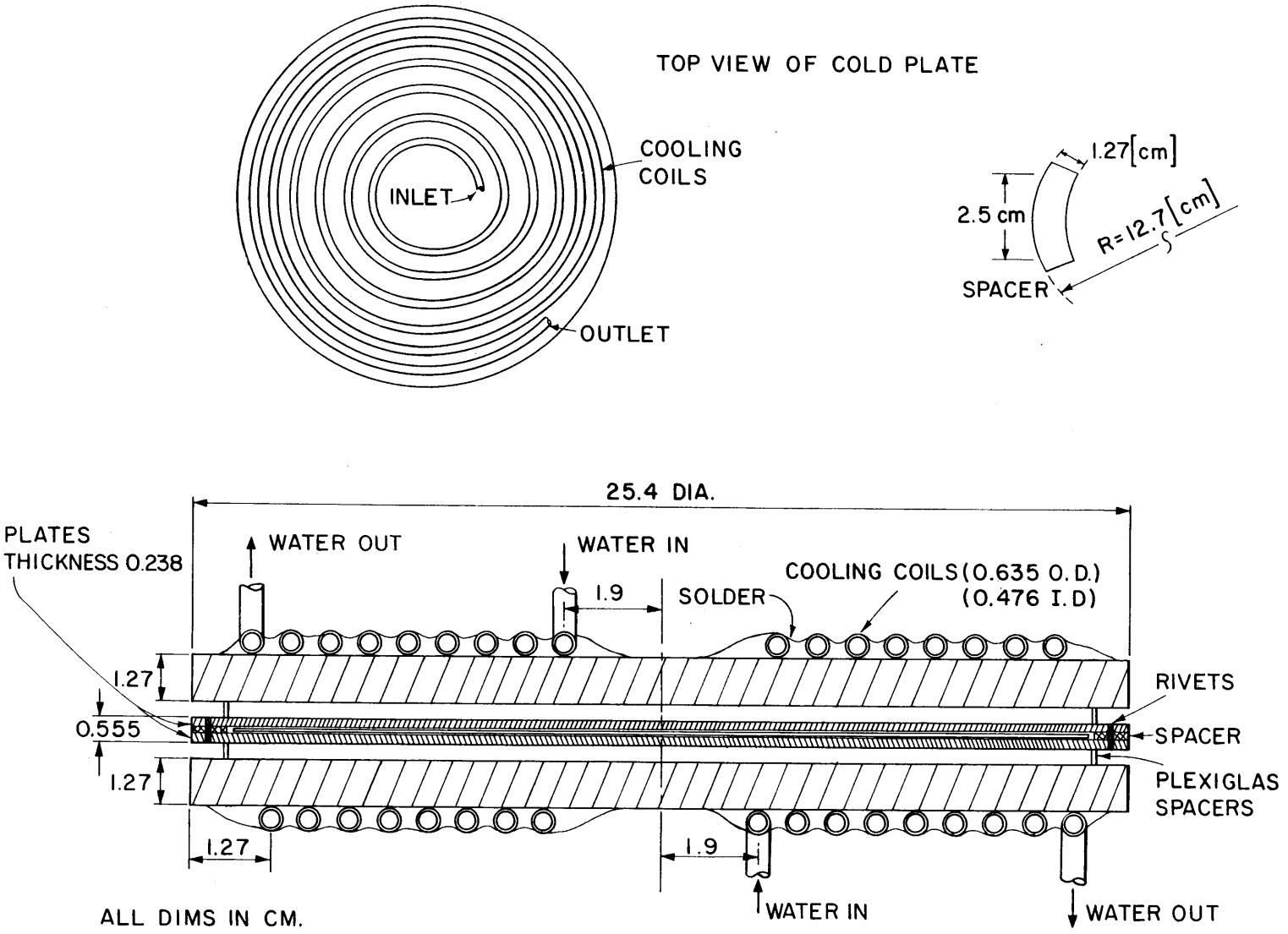

Fig. 3.2 Schematic of the Hot and Cold Plate Assembly

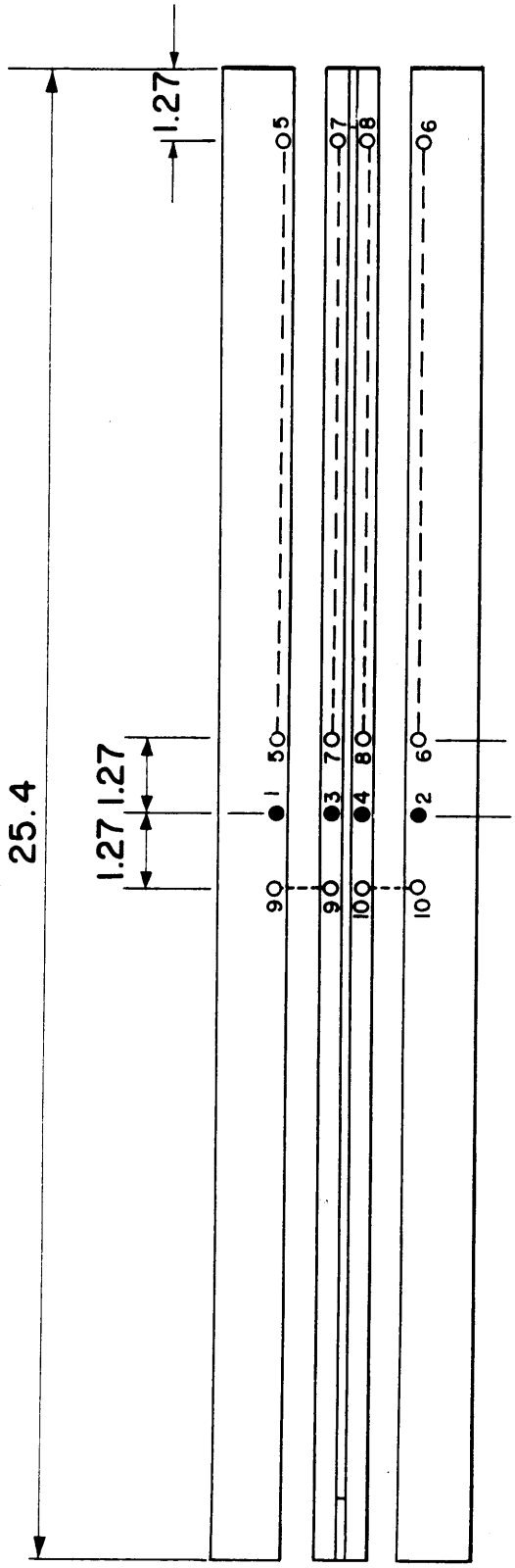

Fig. 3.3 Position of the Thermocouples

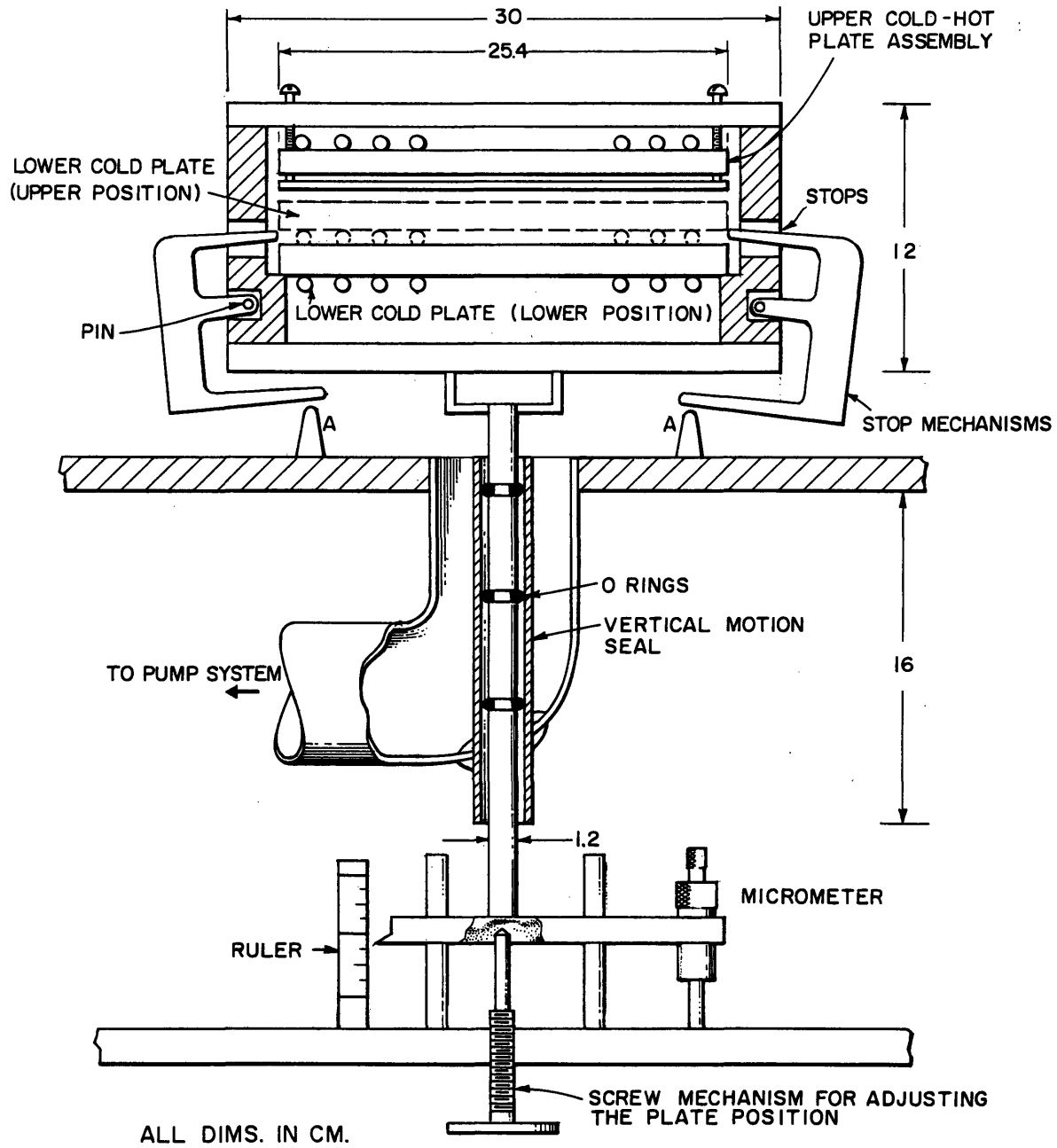

Fig. 3.4 Plate Assembly Positioning System

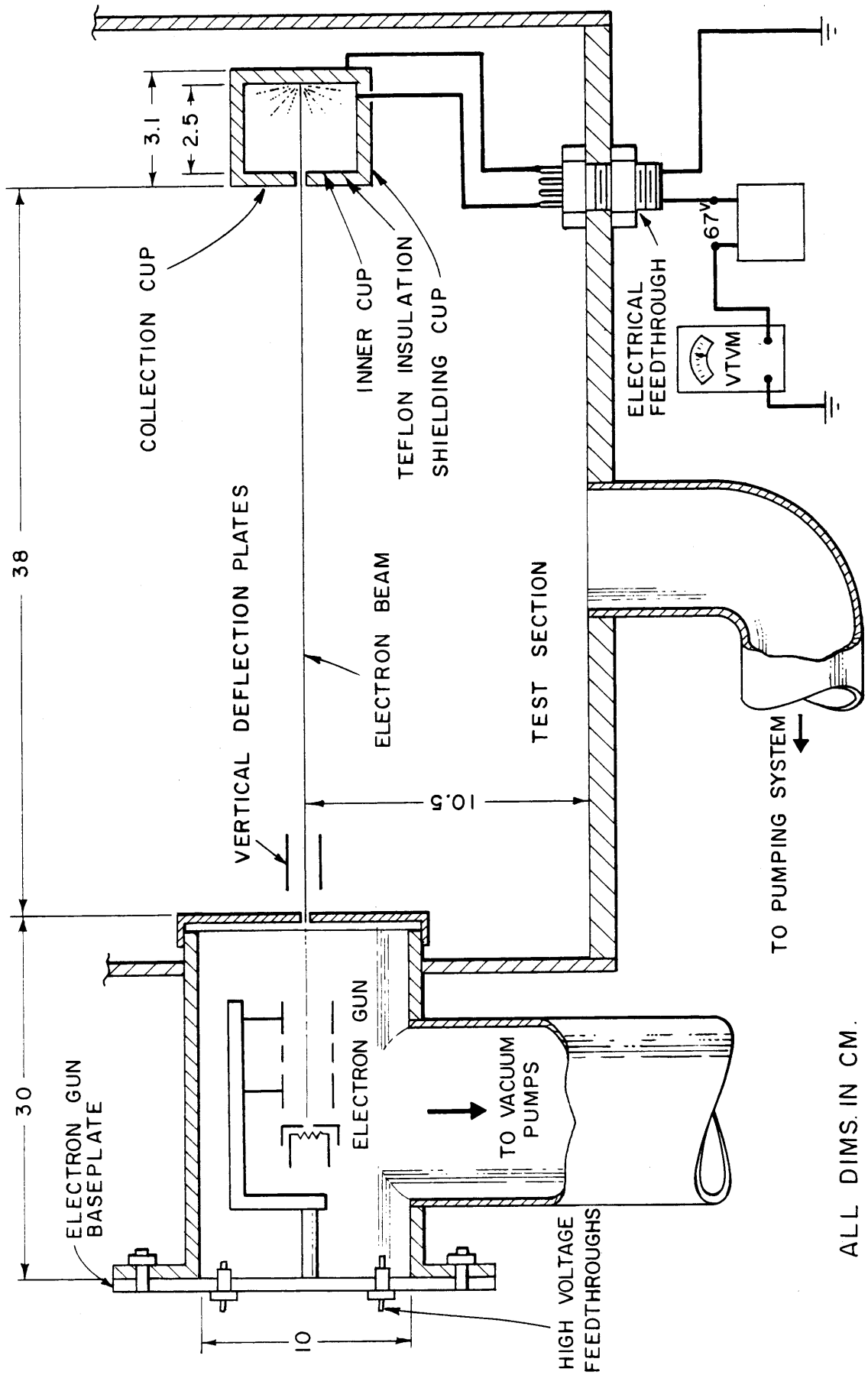

Fig. 3.5 Schematic of the Electron Gun System

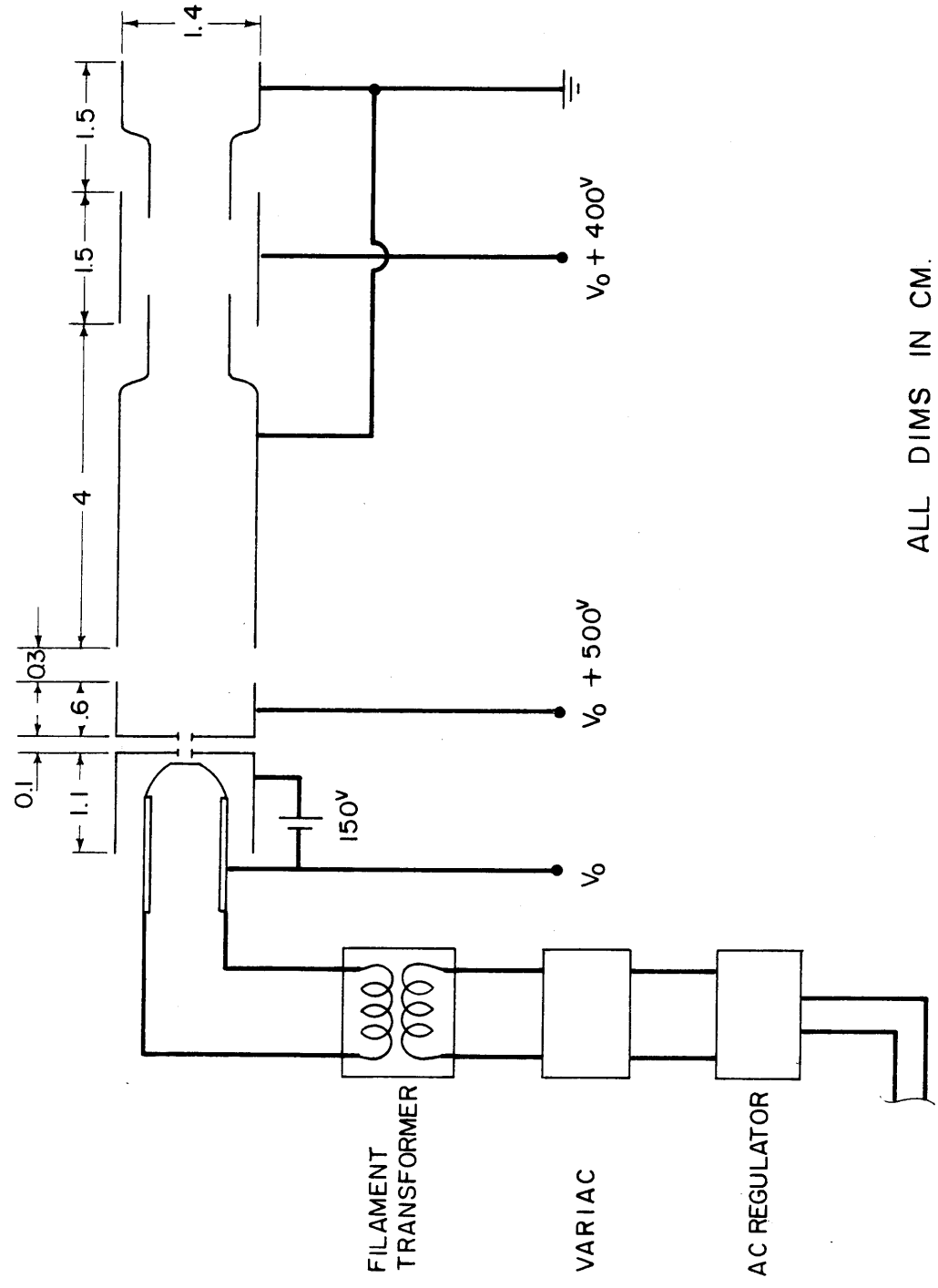

Fig. 3.6 Schematic of the Electron Gun with Typical Operating Voltages

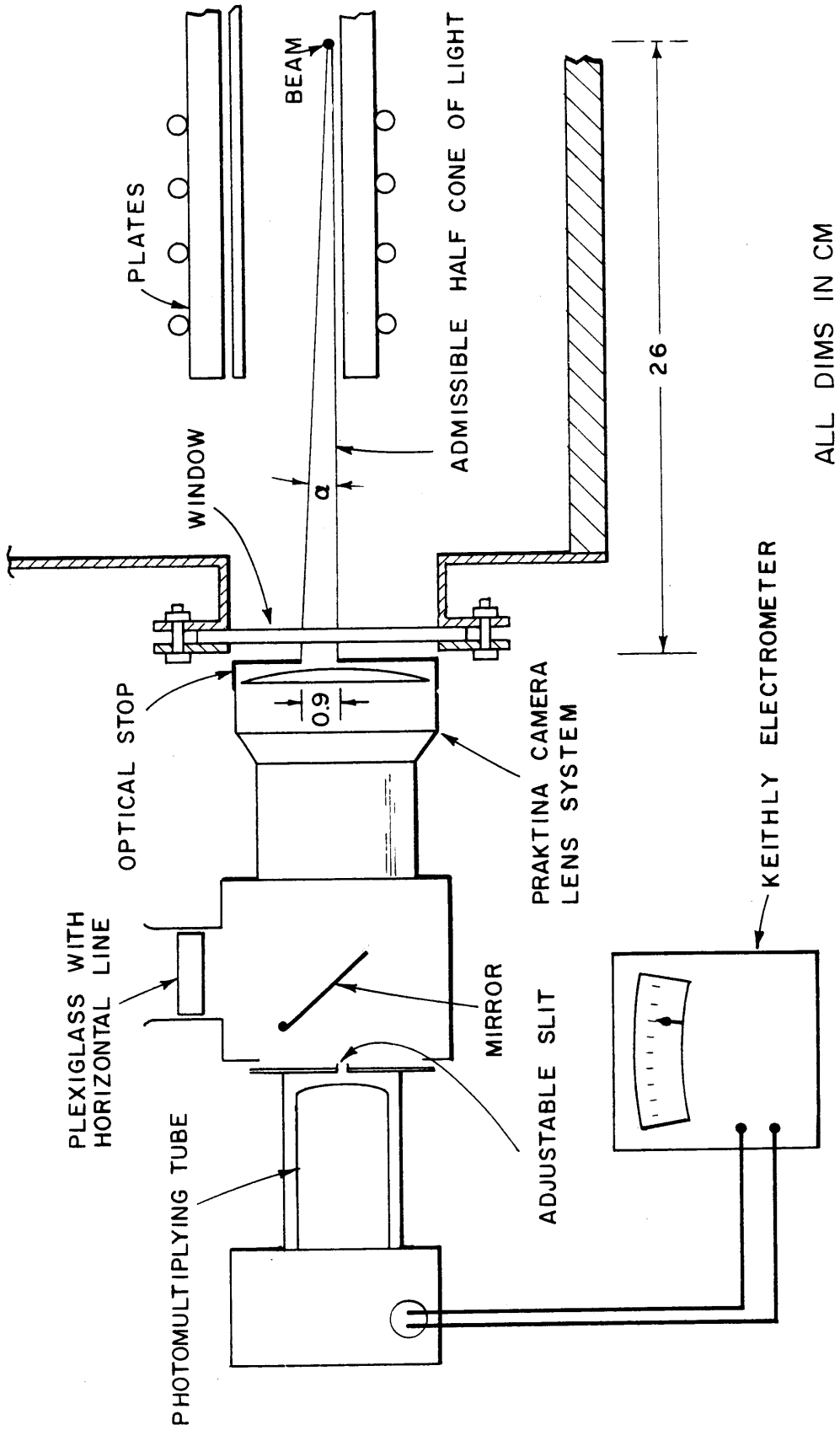

Fig. 3.7 Schematic of the Optical-Photomultiplier System

IV EXPERIMENTAL PROCEDURE

4.A. Heat Transfer:

The heat transfer between the plates was determined by measuring the electrical power input into the hot plate heating element. At any given pressure, measurements were taken only after steady state conditions had been reached. The time required to achieve steady state conditions varied from about five hours for the higher pressure readings to approximately fifteen hours for the free molecule readings.

The total power input (Q_t) was assumed to be the sum of the heat conducted by the gas (Q), the heat transfer due to convection (Q_c), the heat loss due to radiation (Q_r), and the heat conduction through the supports (Q_s). The sum of the latter two losses ($Q_r - Q_s$) was determined at various hot and cold plate temperatures by measuring the power input to the hot plate in vacuum ($(5)10^{-6}$Torr . The heat conduction through the gas was calculated from the expression:

$$Q = 1/2\ (Q_t - Q_v) \qquad (4.1)$$

where $Q_v = Q, + Q_s$. Implicit in Equation (4.1) are the assumptions a) that Q_v is independent of pressure, b) that convection effects are negligible and c) that the same amount of heat is transferred to the top and bottom cold plates.

The validity of the assumption that the convection heat transfer is negligible was ensured by making the plate spacing rather small (0.1348 cm.). The validity of assumption (c) was borns out by temperature measurements between the hot plate and the upper and lower cold

plates.

Figures 5.1 and 5.2 show experimental plots of the thermal conductivity ($\frac{D}{A\Delta T}$ Q) versus the pressure (p). In order to determine these quantities it was necessary to measure:

(a) The power input to the hot plate by measuring the potential drop across the heating element and the potential drop across a standard one-ohm resistance placed in series with the heating element.

(b) The plate temperatures by means of the thermocouples described in Section 3.B.

(c) The pressure level by means of the McLeod gage.

4.B. Density Distribution:

The luminescence produced by the passage of a narrow, high energy electron beam through a rarified gas has been used by a number of investigators[24-29] to measure the density distribution in rarified gas flows. Several of these references, particularly that of Muntz, give rather detailed description of the physics underlying the use of electron beam excited luminescence to measure gas density, and rotational and vibrational temperatures. Here, only a brief description is given on the use of an electron beam for measuring rarified gas densities. It is necessary to have a basic understanding of the principle of operation of an electron beam probe, in order to appreciate the physical limits of its operation and, also, the possible experimental error associated with its use.

When high energy electrons pass through a rarified gas, they undergo collisions with the gas molecules. The collisions may be either elastic or inelastic depending on the total kinetic energy of the interacting pair after the collision. An elastic collision leaves the internal energy of thermolecule unchanged. Such collisions contribute primarily to the spreading of the beam. During an inelastic collision, the high energy electron imparts some of its kinetic energy to the internal energy of the molecule and the molecule ends up in an electronically excited state. The excited state can be either an excited ionization state or an excited state of the neutral molecule. During the transition from the excited state back to the ground state, the molecule (or ion) may emit visible radiation. It is this radiation which is responsible for the luminescence observed to be coincident with the electron beam. The particular excitation-emission process, along with the intensity and spectral characteristics of the resultant luminescence, depends on the nature of the test gas for a given electron beam energy. For nitrogen the radiation is due primarily to the first negative emission system of the ionized nitrogen molecule (N_2+) which occurs at 3914 Å. The first and second positive systems of neutral molecule (N_2) are also observed, although to a much smaller degree. For Argon, Robben and Talbot,[27] observed that the radiation came principally from AI and AII between 3,000 and 4,000 Å.

The intensity of the luminescence from a given volume element along the beam is, under certain conditions of beam energy and gas density, which are described below, proportional to the local number density, i.e.

$$I_L = K\, I_b N$$

where

I_L = intensity of luminescence

K = proportionality constant which is a function of beam energy and the test gas

I_b = electron beam current

N = local molecular number density

If the beam current is maintained constant, then a knowledge of I_L can be used as a measure of N. This relation is valid as long as the luminescence is linearly proportional to the number density. The primary reason for the departure from linearity is probably due to the fact that at higher pressures, not all the excited molecules (or ions) return to their ground state by a direct emission process. At higher pressures, a significant portion of the excited molecules (or ions) collide with another molecule before returning spontaneously to their ground electronic state. During such a collision, the excited molecule can give up its excess energy by a non-radiative process. This process is called collision squelching.

The problem of collision squelching is most pronounced for the longer lived excited states and, therefore, several investigators[24,27,28] have used some form of spectral resolution in order to limit the observed radiation to that due to know show lived states. Both Petrie[28] and Muntz[24] show calibration curves which indicate a linear relationship of intensity versus pressure for the first negative band of N_2 for pressures

up to several hundred microns. The results of Robbin and Talbot[27] indicated that the upper limits of pressure at which the linear relationship between luminescence and pressure holds were 250 microns and 350 microns for argon and nitrogen respectively when using a Corning 7-57 blue filter before the photomultiplier.

Since all the measurements for the present invesitgation were taken at pressures from 3 to 35 microns, it was considered unnecessary to spectrally resolve the beam luminescence.

The limitations placed on the beam voltage are due mainly to the fact that the collision cross sections for electron-molecule interactions are a strong function of the electron energy. The electron collision cross sections increase with decreasing electron energy. If very high voltages are used, the collision cross section may decrease to the point where few inelastic collisions occur and, therefore, the intensity of the luminescence becomes unacceptably low. If very low voltages are used, the electron collision cross section may become so large that the beam experiences excessive spreading or attenuation due to the elastic scattering of the electrons. Previous investigations have worked with beam voltages from 10KV to 50KV. In general, the higher voltages are required for the higher pressures in order to keep beam spreading and attenuation to a minimum. For the present invesitgation, a beam voltage of 10KV was used since all data was taken at relatively low pressures between 3 and 40 microns. Under these conditions of voltage and pressure the spreading and attenuation of the beam were found to be negligible. This was determined by noting that no measurable change in the measured beam current was detected while the

beam traversed the space between the plates under plate temperature and pressure conditions such that the density change between the plate centerplane and the cold plate was about 8 percent. (i.e. about the maximum density change used during the experiment.)

The present experiment was performed by sending a narrow, constant current beam of high energy electrons between the plates and parallel to them. The luminescence from a given length of beam was then focused by an optical system onto the face of a photomultiplier. The output of the photomultiplier was assumed to be proportional to the number density of molecules at that position of the beam. The plates were moved vertically relative to the beam so that photomultiplier readings were obtained for a range of beam positions relative to the plates. All photomultiplier readings were normalized relative to the centerplane reading and the density profile was assumed to be:

$$\frac{N(x)}{N_o} = \frac{I(x)}{I_o} \tag{4.2}$$

where I_o was the centerplane reading and $I(x)$ the reading at any position x. The density ratio, $N(x)/N_o$, is the quantity evaluated from the linearized analytical results and, therefore, the experimental results could be compared directly with the analytical results.

Before the density distribution curves were measured, a heat transfer measurement was taken in the free molecule regime with a plate spacing of 0.1348 cm. This measurement was compared with the heat transfer vs pressure curves taken previously to ensure that the accommodation coefficient had not changed. For both test gases, it was

found that the accommodation coefficient remained a constant. A knowledge of the accommodation coefficient was necessary so that the experimental results could be compared to the analytical results.

V. EXPERIMENTAL RESULTS - HEAT TRANSFER

Experiments were performed using argon, nitrogen and air as test gases. The argon and nitrogen were available commercially in cylinders (Airco) and no attempt was made to further purify them. Air was supplied directly to the system from the atmosphere. The aluminum plate system was used with argon and nitrogen and the copper plate system with air.

Plots of $\frac{D}{A\Delta T}Q$ vs. D/λ are shown in Figures 5.1 and 5.2. These plots show clearly the free molecular and transition regimes.

Continuum Thermal Conductivity

An important test of the accuracy of the heat transfer measurements was their ability to yield correct values of the continuum thermal conductivity. The continuum thermal conductivities of argon and nitrogen were evaluated using a plot similar to that employed by Thomas and Golike.[11] In this method measured values of $\frac{A\Delta T}{DQ}$ are plotted against the corresponding reciprocal pressure, 1/p. The continuum thermal conductivity is obtained by extrapolating the plot to $1/p = 0$. These reciprocal plots for argon and nitrogen are shown in Figures 5.3 and 5.4. The value for the thermal conductivity for air was obtained by directly measuring the heat transfer at atmospheric conditions.

The continuum thermal conductivities are listed in Table 1. In this table reference values quoted from the literature are also given.

A comparison between the measured and the reference values shows good agreement, the largest difference between them being 3.5 percent for air when the distance between the plates was 0.32 cm. When the distance between the plates was reduced to 0.1348 cm. the difference between the measured and reference values decreased to about 1.5 percent indicating possible convection effects at the larger plate separation. All heat transfer data for argon and nitrogen was taken at the smaller plate spacing.

Thermal Accommodation Coefficients:

In order to compare the experimental results for both heat transfer and density distribution with those of analysis it is necessary to measure values of the accommodation coefficient for the various test gas-surface combinations used. For argon and nitrogen the accommodation coefficient was determined from the heat transfer measurements made in the pressure ranges corresponding to both the free molecule and temperature jump regimes.

Free Molecule Accommodation Coefficient:

At low pressures, where the mean free path (λ) molecules in the gas is large compared to the separation between the plates (D), the gaseous heat conduction per unit area (A) and unit temperature difference ($\Delta T = T_H - T_C$) is given by Knudsen's formula:[23]

$$Q/A\Delta T = \Lambda_o \frac{\alpha}{2-\alpha} \; p \left(\frac{273.2}{T_C} \right)^{1/2} \qquad (5.1)$$

where p is the pressure in microns and Λ_o is the free molecule conductivity at 0°C. Its value for argon is 9.29 watts cm^{-1} dg^{-1} $micron^{-1}$ and for nitrogen is 16.63 watts cm^{-1} dg^{-1} $micron^{-1}$. In writing equation (5.1) it was assumed that the accommodation coefficients for the hot and cold plates are equal ($\alpha=\alpha_C=\alpha_H$) and that they are uniform across the plate surfaces. The thermal accommodation coefficients (α_{LP}) evaluated from equation (5.1) for the experimentally determined values of Q, A, Tc, Tm and p are listed in Table II for argon and nitrogen. The data indicates that the scatter in the measured values of α was ±2 percent from the mean value for both gases.

Temperature Jump Accommodation Coefficient:

When the gas is only slightly rarified the heat conduction per unit area and unit temperature difference may be written as:[22]

$$\frac{Q}{A\Delta T} = \frac{\bar{k}}{D + g_C + g_H} \tag{5.2}$$

Where the temperature jump distance is:

$$g = \frac{2-\alpha}{\alpha} (2\pi RT)^{1/2} \frac{\bar{k}}{(\gamma+1)C_v p} \tag{5.3}$$

In equation (5.3), R is the gas constant, γ the ratio of specific heats and C_v the specific heat at constant volume. By taking T as the average temperature between the hot and cold plates and by assuming $g = g_C = g_H$ equations (5.2) and (5.3) may be rearranged to yield:

$$\frac{A\Delta T}{D} \frac{1}{Q} = \frac{1}{\bar{k}} + \left[\frac{2-\alpha}{\alpha} \frac{(8\pi RT)^{1/2}}{D(\gamma+1)C_v} \right] \frac{1}{p} \tag{5.4}$$

Thus, a thermal conductivity coefficient, α_{TJ}, can be calculated by equating the slope of the reciprocal plot described previously (see Fig. 5.3 and 5.4) to the bracketed expression in equation (5.4). The resultant α_{TJ} values are shown in Table II. The difference between α_{TJ} and $\bar{\alpha}_{LP}$ is 3.9 percent for argon and 7.8 percent for nitrogen. This agreement is good compared to the large discrepancies often found between accommodation coefficients determined by the free molecule and temperature jump methods.[11,15] A possible reason for this relatively good agreement might be that the parallel flat plate geometry minimizes the convection problems which often occur with a cylindrical geometry at higher pressures.

Comparison of Experimental Results with Analysis:

In Figures 5.5 and 5.6 the experimental values of $\frac{Q}{Q_{FM}}$ vs D/λ for argon and nitrogen are plotted along with the analytical results available for $\alpha \neq 1$. The values of accommodation coefficients used in evaluating the analytical results are those calculated from the free molecule heat transfer. The value of Q_{fn} is also calculated using this value of accommodation coefficient. The analytical $\frac{Q}{Q_{fm}}$ curve for nitrogen is that calculated from the "modified" Lees results (Appendix II).

The results for argon indicate that the full range, four-moment results of Lees and Gross-Ziering give good agreement with experiment. The only higher approximations available for $\alpha \neq 1$ are the 8-moment methods of Gross and Ziering. These results fall considerably below

(10 - 20 percent) the experimental results. For reasons which are not clear, the eight-moment half range results of Gross and Ziering are not sensitive to changes in the accommodation coefficient. For example, for the eight-moment, hard sphere case, changing the accommodation coefficient from 1 to 0.8 results in a change for the heat transfer ratio from 0.395 to 0.41, or by about 3.8 percent for a D/λ value of 5. For the Lees four-moment results a similar change in the accommodation coefficient results in the heat transfer ratio changing from 0.435 to 0.525, or about 20 percent, again at $D/\lambda = 5$. A similar insensitivity to changes in the accommodation coefficient is also evident for the density profiles obtained from the eight-moment results. It is mainly this insensitivity to changes in the accommodation coefficient which is responsible for the disagreement between the four-moment and eight-moment results becoming more pronounced for lower values of the accommodation coefficient.

Unfortunately, none of the non-linear theories considered[4,5,6] were carried out for values of accommodation coefficient other than unity. For this reason, these results can not be compared directly with the experimental results. It can be noted, however, that for $\alpha = 1$ the non-linear results fall close to the four-moment linear results. Hence a generalization of the non-linear methods to allow for arbitrary values of the accommodation coefficient may be worthwhile.

Plot 5.6 indicates that the modified Lees results give very good agreement (± 2 percent) with experiment for nitrogen. This agreement is an indication that the assumptions used in modifying the Lees results to apply to diatomic molecules are not too much in error.

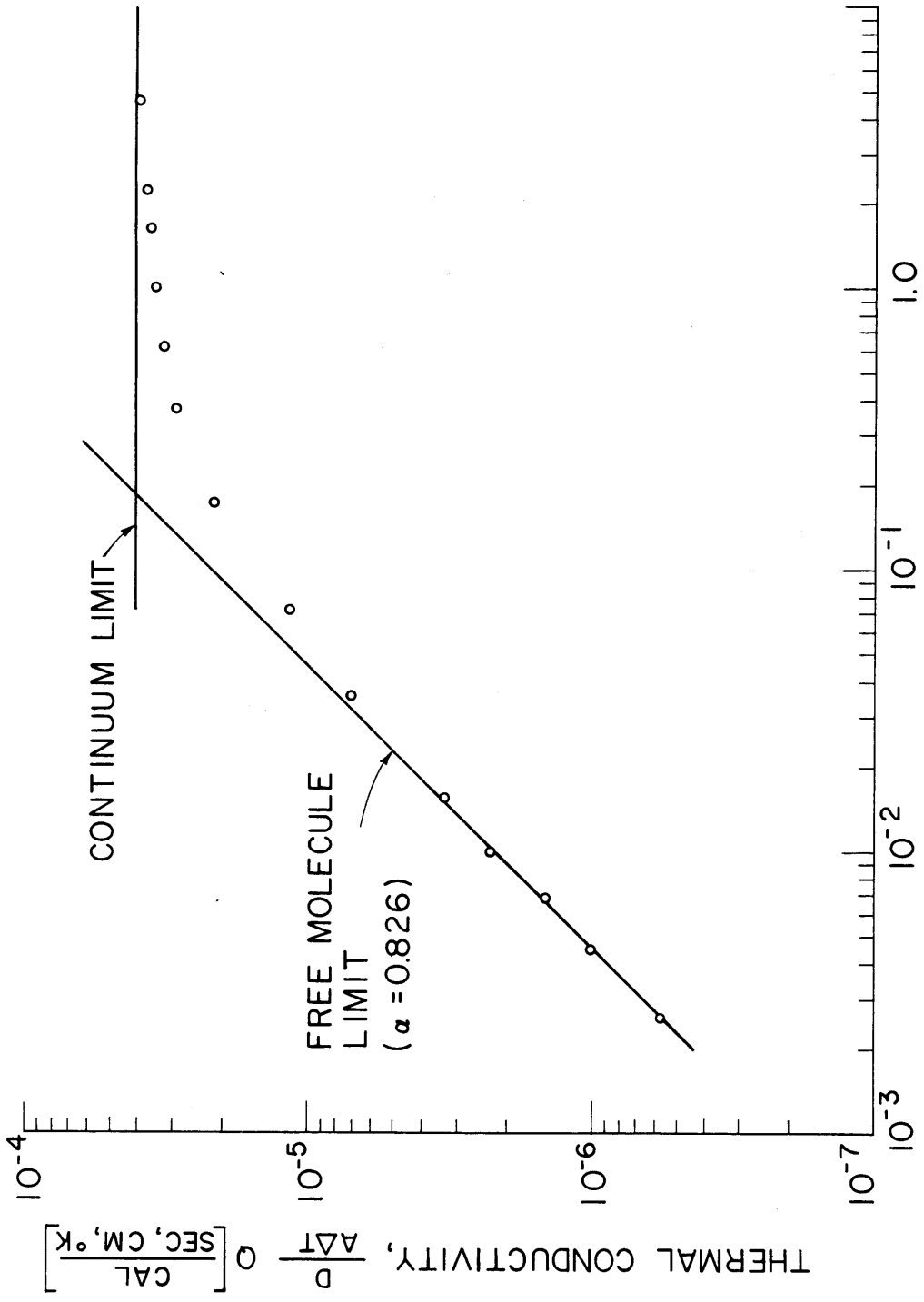

Fig. 4.1 Heat Transfer Versus Pressure Plot for Argon

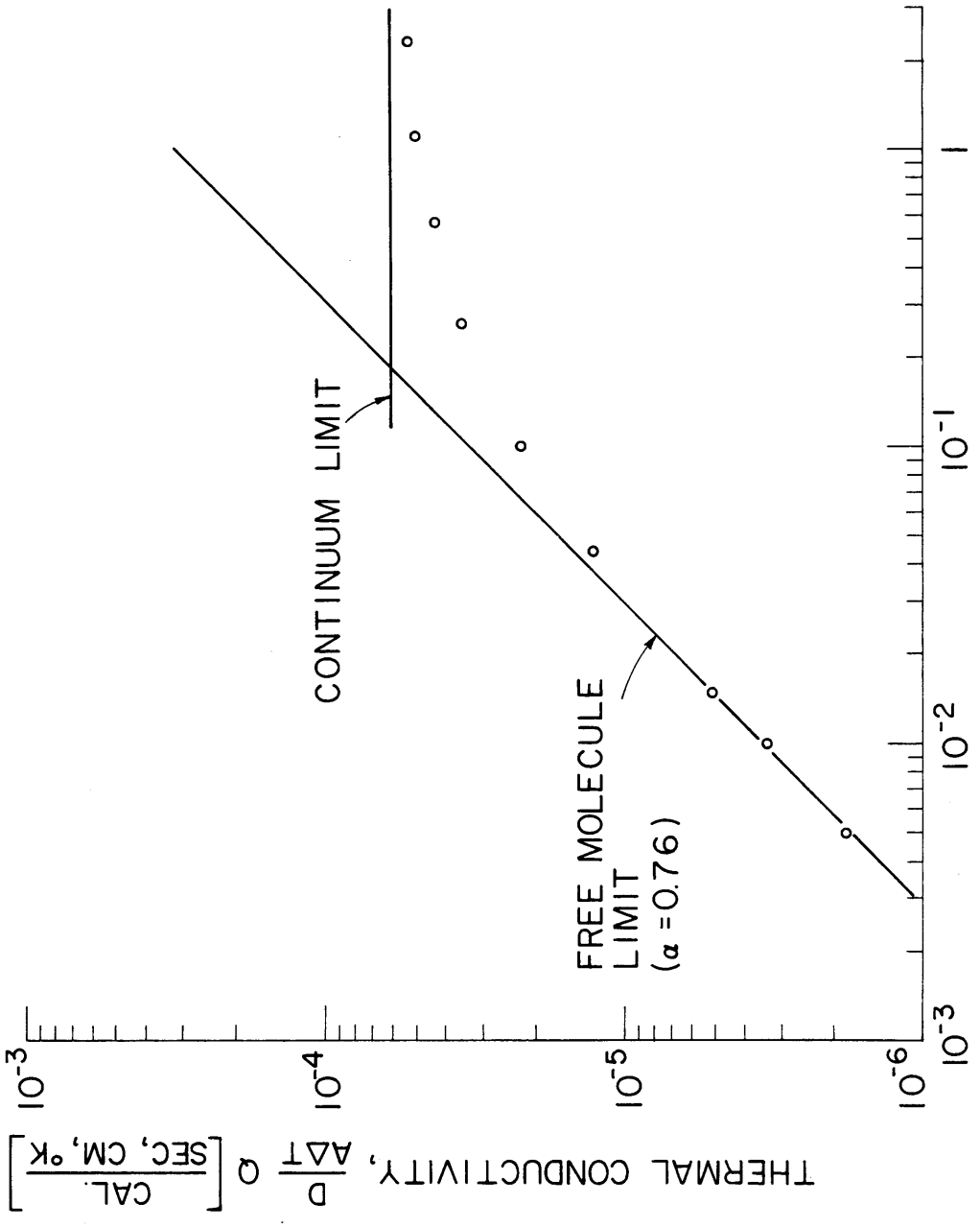

Fig. 4.2 Heat Transfer Versus Pressure Plot for Nitrogen

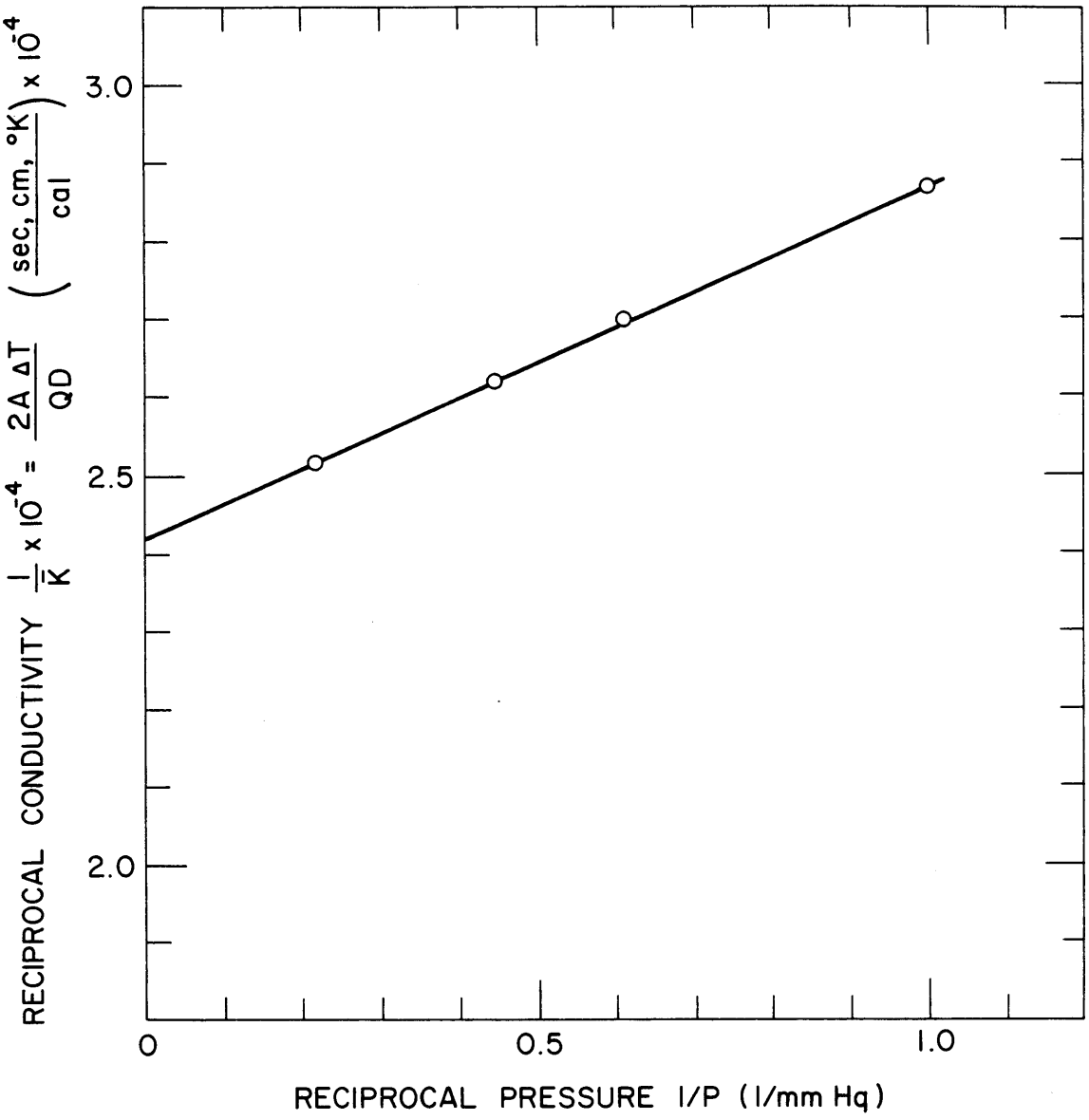

Fig. 4.3 Reciprocal Plot for Argon

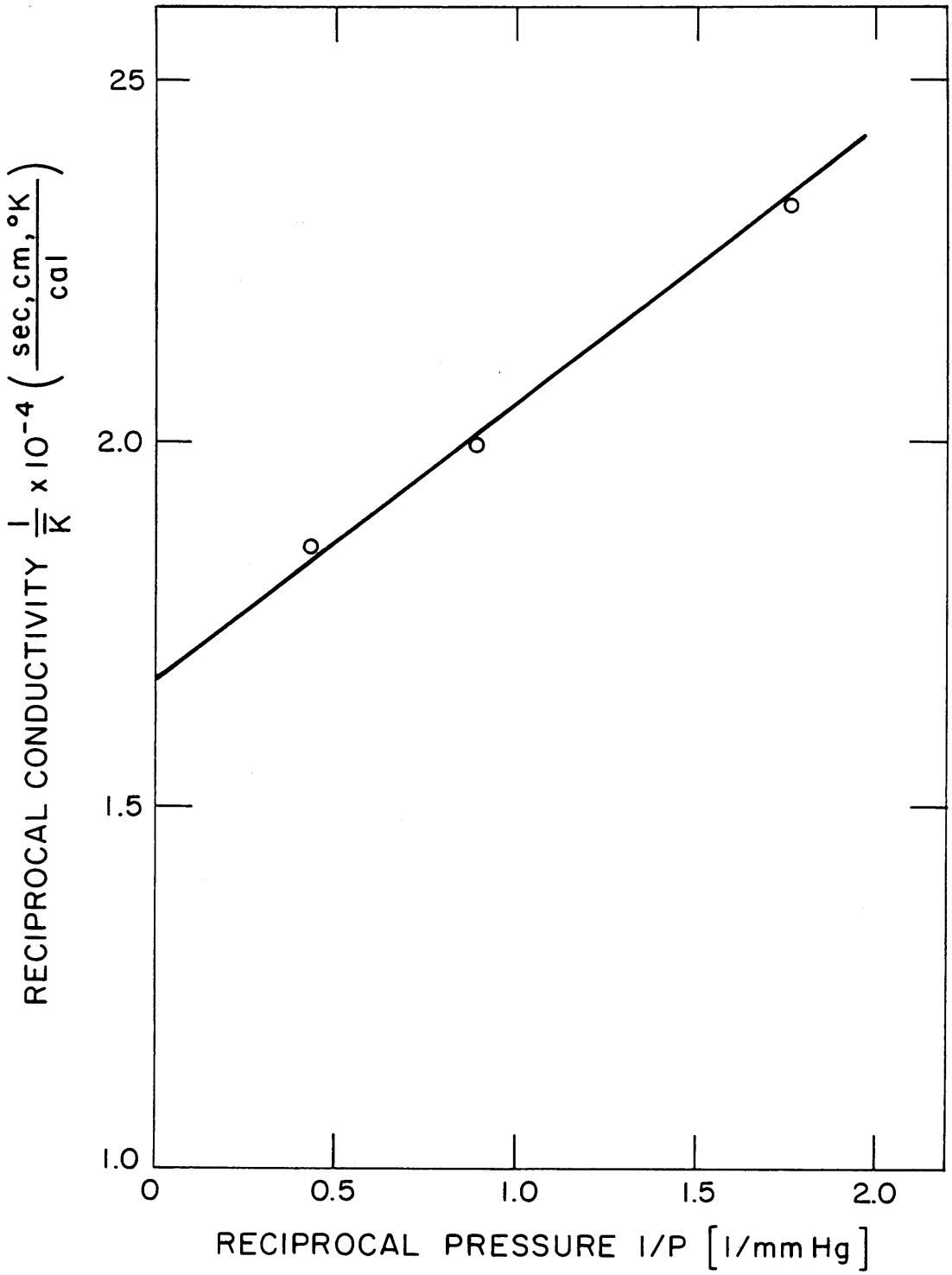

Fig. 4.4 Reciprocal Plot for Nitrogen

TABLE I. Thermal Conductivities of Argon, Nitrogen and Air at One Atmosphere

Gas	Plate Gap(d) (cm)	Temperature °K			Thermal Conductivity	cal/sec,cm, °K x 10^7
		T_H	T_c	T_{avg}	Measured	Reference Value*
A	0.1445	299.4	294.8	297.1	414	415[a]
N_2	0.143	301.96	293.41	297.68	602	585[b]
						621[c]
Air	0.1348	288.06	280.11	284.08	575	584[d]
	0.320	290.89	280.06	285.47	608	587[d]

*) These values were obtained by interpolating the data, given for the temperatures $T_{avg} = (T_H + T_c)/2$, by

a) Tsederberg, Ref. 14, page 84

b) Euken, as quoted by Tsederberg, Ref. 14, page 91

c) Vargaftik, as quoted by Tsederberg, Ref. 14, page 126

d) Taylor and Johnston, Ref. 21

TABLE II. Thermal Accommodation Coefficient for Argon On Aluminum as Determined by the Low Pressure and Temperature Jump Methods.

Pressure mm Hg x 10^3	α_{LP}
2.6	0.830
4.5	0.831
6.8	0.810
10.0	0.832
	$(\alpha_{LP})_{avg}$ = 0.826

From the reciprocal plot

(Fig. 5.3) and Eq. 5.4 α_{TJ} = 0.795

Thermal accommodation coefficient for nitrogen on Aluminum as determined by the low pressure and temperature jump methods

Pressure mm Hg x 10^3	α_{LP}
5	0.775
10	0.749
14.95	0.752
	$(\alpha_{LP})_{avg}$ = 0.759

From the reciprocal plot

(Fig. 5.4 and Eq. 5.4 α_{TJ} = 0.705

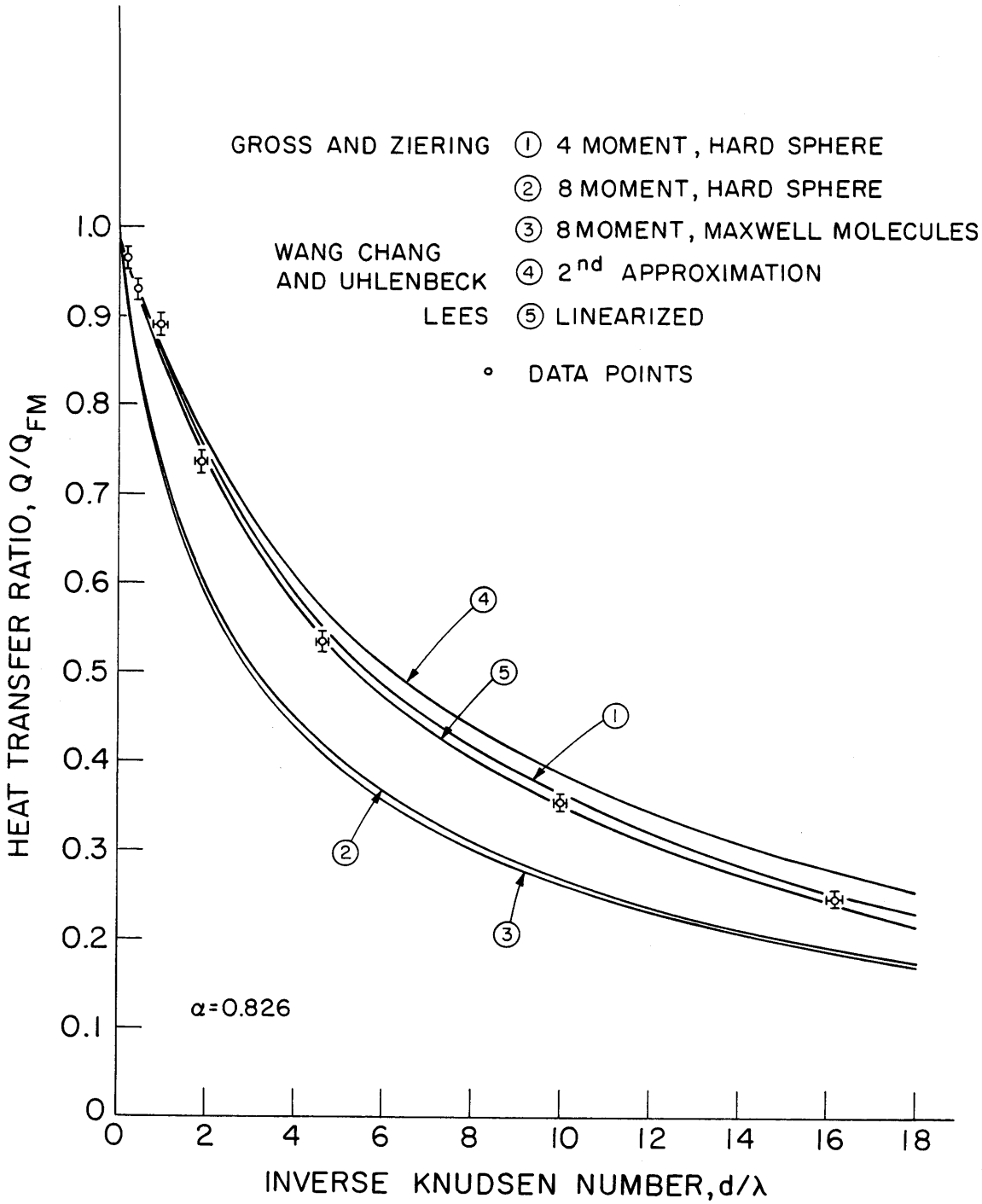

Fig. 4.5 Heat Transfer Ratio Versus Inverse Knudsen Number - Comparison Between the Experimental Argon Results and the Results of the Analyses

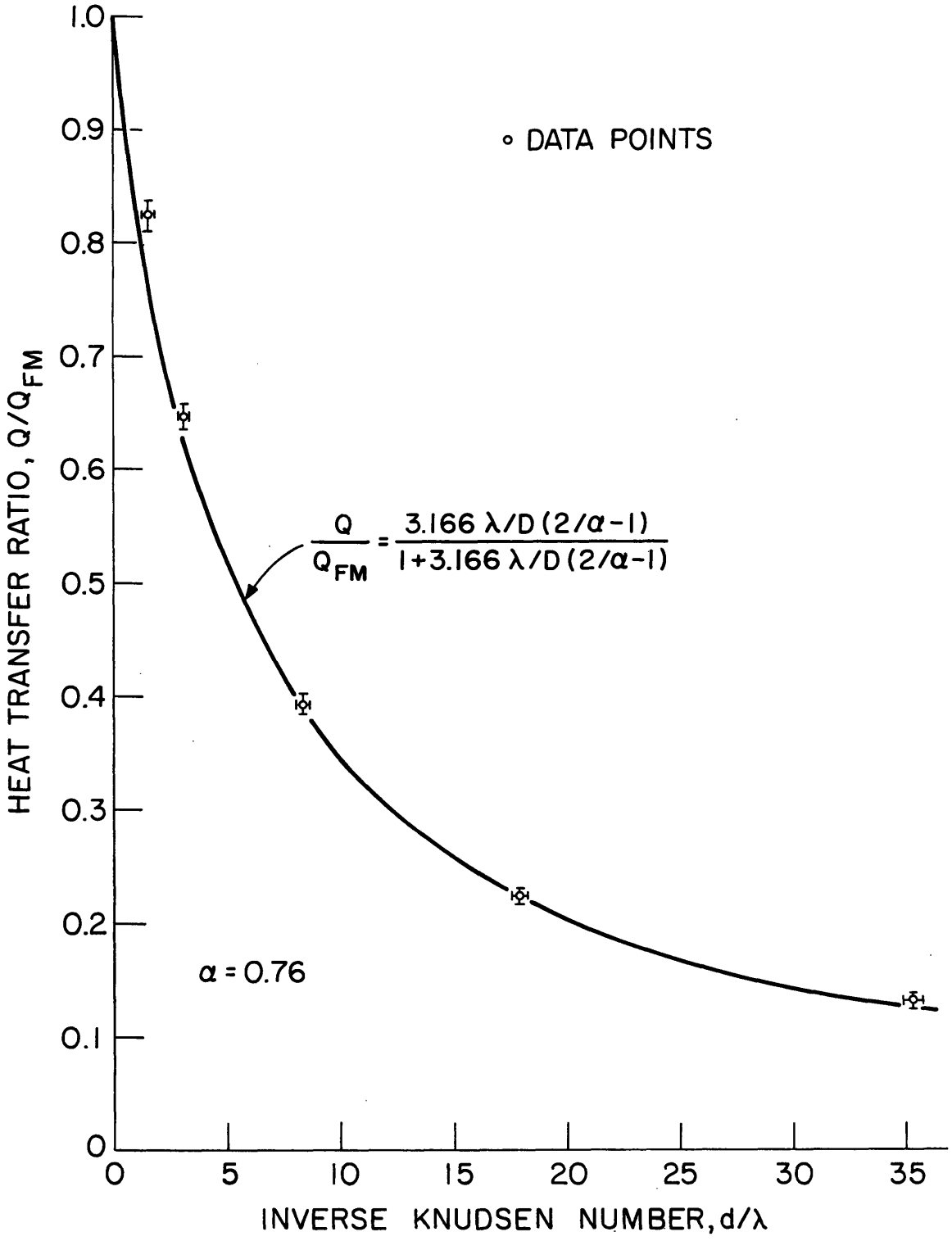

Fig. 4.6 Heat Transfer Ratio Versus Inverse Knudsen Number - Comparison Between Experimental Nitrogen Results and the Results of the Lees' Moment Method

Experimental Errors - Heat Transfer:

The errors associated with the heat transfer measurements are estimated to be ±3.0 percent. The sources of error can be divided up into roughly three types, these being:

(1) Edge and convection effects

(2) Non-uniform temperature distributions across the plates

(3) Instrumental errors.

These three types of errors are described below:

Edge and Convection Effects:

A calculation of the Grashof number (Gr - 0.2) at atmospheric pressure indicates that the effects of convection are negligible for the small plate spacing and temperature differences used. Since one expects convection effects to be most likely at atmospheric pressure, such effects can be considered to be negligible as a source of error for these experiments.

The errors due to edge effects have been kept low by making the ratio of plate spacing to plate diameter large (2,000). Under continuum conditions, edge effects can be expected to be present to about one plate spacing in from the outer edge. The ratio of the plate area effected by edge effects to total plate area is then about 1/50. A reasonable estimate of the error due to edge effects is about 1 percent since, even in the area effected by edge effects, heat is being transferred between the two plates.

Effects Due to Non-uniform Temperature Distributions:

It was very important to maintain each plate at a uniform temperature. Difference thermocouples were provided to determine temperature differences between the center and outer edge of the plates. For all pressures this difference was negligible for the cold plates. For low pressures it was negligible for the hot plate. At higher pressures, (near continuum) when a rather large amount of power was supplied to the hot plate, temperature differences between the center and outer edge of the plate of about 1/4°F were observed. This indicates uncertainty in the determination of hot plate temperature of about 1/8°F. With ΔT being at least 15°F, the error from the source is about 3/4 percent of higher pressures.

Instrumental Errors:

Instrumental errors can arise from several causes, the most important being inaccurate pressure, temperature, and power input values. These sources of error are described below:

Pressure Readings:

The pressure was determined by readings from a McLeod gage. The accuracy of readings from a McLeod gage changes with pressure. For the low pressure levels corresponding to the free molecule measurements ($p \doteq 10$ microns), the estimated uncertainty in the pressure readings was ±3 percent. For pressure levels corresponding to the transition regime ($p = 70$ microns), the estimated uncertainty in the pressure readings was estimated to be ±1.5 percent. These estimates of error

were made by noting that the manufacturer's (Todd Scientific) specifications for the gage indicate an accuracy of ± 0.0001 mm Hg for the scale used. Such an accuracy would indicate errors of from 1 to 0.2 percent for the pressure ranges under consideration. The larger error estimates actually used take into account the difficulty of actually reading a McLeod gage to the ultimate accuracy of the instrument.

Temperature Readings:

The difference in the plate temperatures was determined in two ways: (1) by measuring the plate temperatures directly, and (2) by directly measuring the temperature difference with a difference thermocouple. The agreement between these readings is to within 1/10°F out of 15°F indicating errors on the order of 1/2 percent due to incorrect temperature readings.

Power Input

The instrument (AC-VTVM) measuring the power input to the hot plate was accurate to within 1/3 percent full scale indicating a probable error in the measured power input of about 0.47 percent. The actual accuracy of the VTVM (Hewlett-Packard Model 400D) is about 1 percent full scale, however, this instrument was calibrated several times during the experiment against a voltage supply which has an accuracy of 1/10 percent. The voltage readings of the VTVM were then adjusted to take into account the error indicated by the calibration. It should be noted that the conduction heat transfer is given as $Q = Q_t - Q_v = Q_t\left(1 - \frac{Q_v}{Q_t}\right)$ [Eqn.41]. The power input error shows up both

in the total power input (Q_t) and the power loss in vacuum term (Q_v). At higher pressures the ratio, Q_v/Q_t, is small and, therefore, a small error in Q_v contributes very little to the total error in Q. For example, for pressures corresponding to D/λ values in the lower transition regime ($1 < D/\lambda < 25$), the average value of the ratio, Q_v/Q_t, was about 0.04 indicating a probable error in Q due to the uncertainty in Q_v of about 0.02 percent. In the free molecule regime, however, the average value of the ratio, Q_v/Q_t. was about 0.3. The uncertainty in Q_v, therefore, results in a probable error in Q of about 0.15 percent in the free molecule limit. The uncertainty in the measured power input can, therefore, result in a total error of about 0.65 percent in the free molecule limit and about 0.50 percent in the transition regime.

To arrive at an overall probable error for the measurements from the above discussion, the sources of error should be divided into two groups, these being:

(1) Those which contribute to errors in Q/Q_{FM}

(2) Those which contribute to errors in D/λ

The probable error in the experimental values of Q/Q_{FM} is due to errors in both Q and Q_{FM}. The errors involved in the determination of Q are those due to uncertainty in the power input and the edge effects. Q_{FM} was calculated from the Knudsen expression using experimentally determined values of α, ΔT and p. The error in α is assumed to be equal to the experimental scatted actually observed about the mean value, i.e. $\pm$ 2 percent. The error in Q is thenestimated to be about 1.2 percent.

and that in Q_{FM} about 2.5 percent. These values were arrived at by assuming the errors were independent and using the root mean square method to calculate the standard error, as described by Cook and Rabinowicz,[29] The probable error in the ratio, Q/Q_{fm} was calculated in the same way to be on the order of ± 3 percent.

The probable error in the values of D/λ was due to uncertainties in the pressure readings which were estimated to be ± 3 percent for the lower pressure measurements and ± 1.5 percent for the higher pressure measurements.

The errors associated with the value of the accommodation coefficient could lead to an uncertainty in the position of the four-moment analytical results of about ± 2 percent for D/λ values ranging from 1 to 15.

The errors associated with the experimental values of Q/Q_{fm} and D/λ are indicated in Figures 5.6 and 5.7 by vertical and horizontal error bars.

VI. EXPERIMENTAL RESULTS - DENSITY DISTRIBUTION

Density distribution measurements were made using both argon and nitrogen as test gases. Both gases were used with the aluminum plates. The argon density distribution curves are shown in Figure 6.1 and 6.2 and the nitrogen curves in Figure 6.3. The curve labeled "continuum" corresponds to the plot one would obtain for continuum conditions ($D/\lambda >> 1$). The analytical results were evaluated using the values of accommodation coefficient as calculated from the free molecule heat conduction data of the previous section. After the system had been exposed to atmosphere, these values of the accommodation coefficient were checked by taking a free molecule heat transfer measurement as explained in Section V. It was found that the value of the accommodation coefficient did not change for either test gas during the course of the experiments.

All the data is shown for beam positions going from the midpoint between the plates toward the cold plate (i.e. increasing density). As mentioned at the end of this section, the closest approach possible to the plate was 1.59 cm. During the experiments several measurements were made with the beam approaching the hot plate. These measurements indicated that the density distribution was symmetrical about the plate center plane. This being the case, only half range density distribution measurements are shown.

Argon:

The results for argon indicate that the linear four-moment methods of both Lees and Gross and Ziering along with the second approximation

of Wang-Chang and Uhlenbeck agree rather closely with the data. This agreement is indicated for D/λ values from 1.319 (nearly free molecule) to 15.2 (approaching temperature slip.) The average agreement between the measurements (average value) and the four-moment results is ±3 percent. The only measurement which is in substantial disagreement with the four-moment results is that closest to the cold plate taken at 32 microns (D/λ = 15.2). This point falls about 5.5 percent below the average of the four-moment results. Possible reasons for this discrepancy are suggested in the discussion on sources of error at the end of this section.

The data falls about 6-20 percent below the results of the Gross and Ziering eight-moment methods. As discussed at some length for the heat transfer results, the eight-moment methods are not as sensitive to changes in the accommodation coefficient as the four-moment results would indicate. Rather significant disagreement (30 percent) between the results of the eight-moment and the four-moment methods exists, however, even for the case of an accommodation coefficient of unity for values of D/λ near one.

In Figure 6.2 all the experimental argon density distribution curves are plotted together showing only the average values with brackets indicating the scatter.

Again, the analysis of Frankowski et al,[7] and the non-linear results[4,5,6,7] were carried out only for an accommodation coefficient of unity and, therefore, they cannot be directly compared with the data. For the unity accommodation case, however, the non-linear

results tend toward the four-moment linearized results while the Frankowski results tend toward the eight-moment results.

Nitrogen:

The results for nitrogen are shown in Figure 6.3. These profiles are very similar to those for argon, inasmuch as they indicate an increasing "density slip" with decreasing pressure and are, to within the limits of the scatter, linear.

Unfortunately, there were no analytical results available with which to compare the nitrogen density distribution measurements.

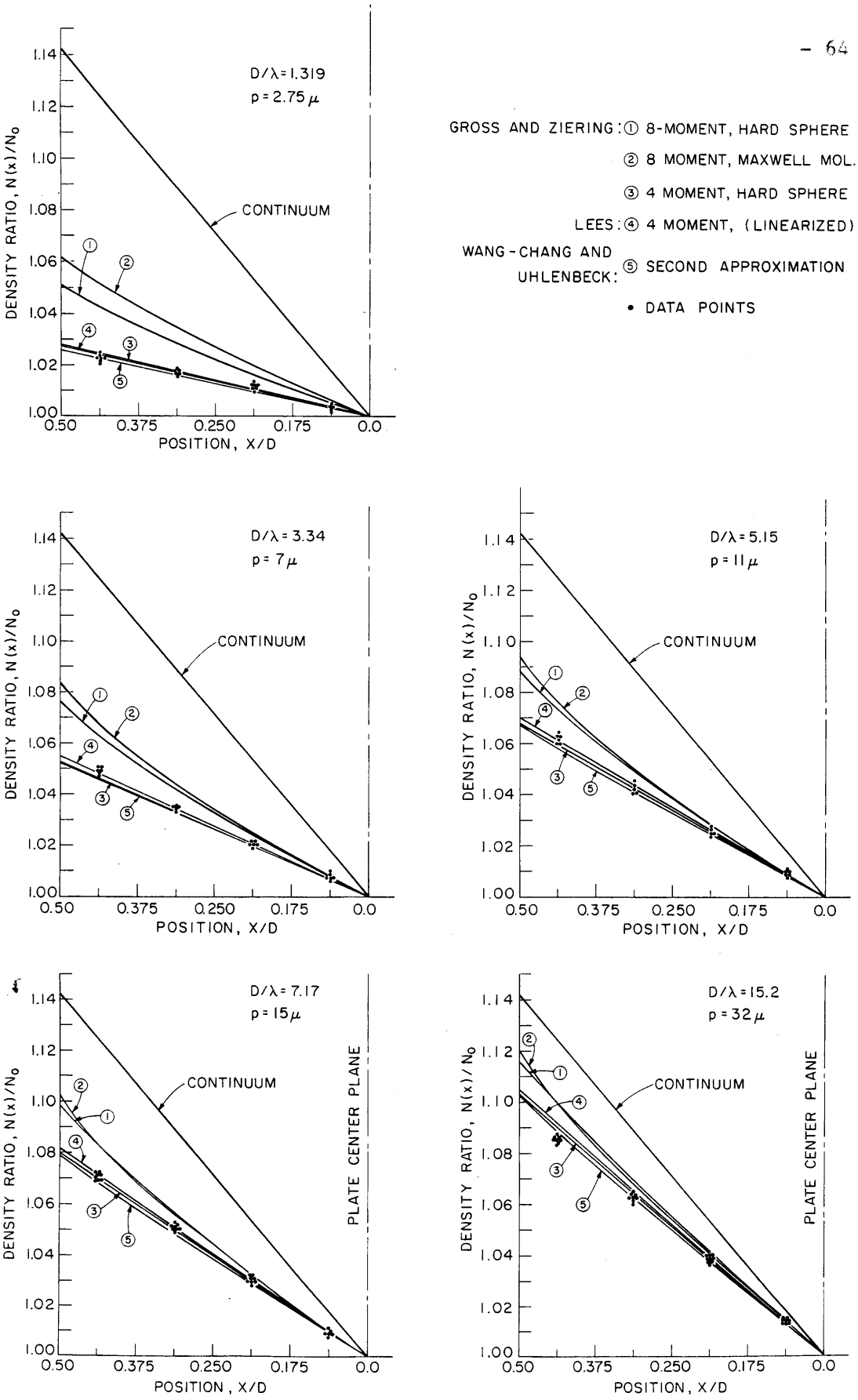

Fig. 5.1 Density Ratio Versus Position - Comparison Between Experimental Argon Results and the Results of the Analyses

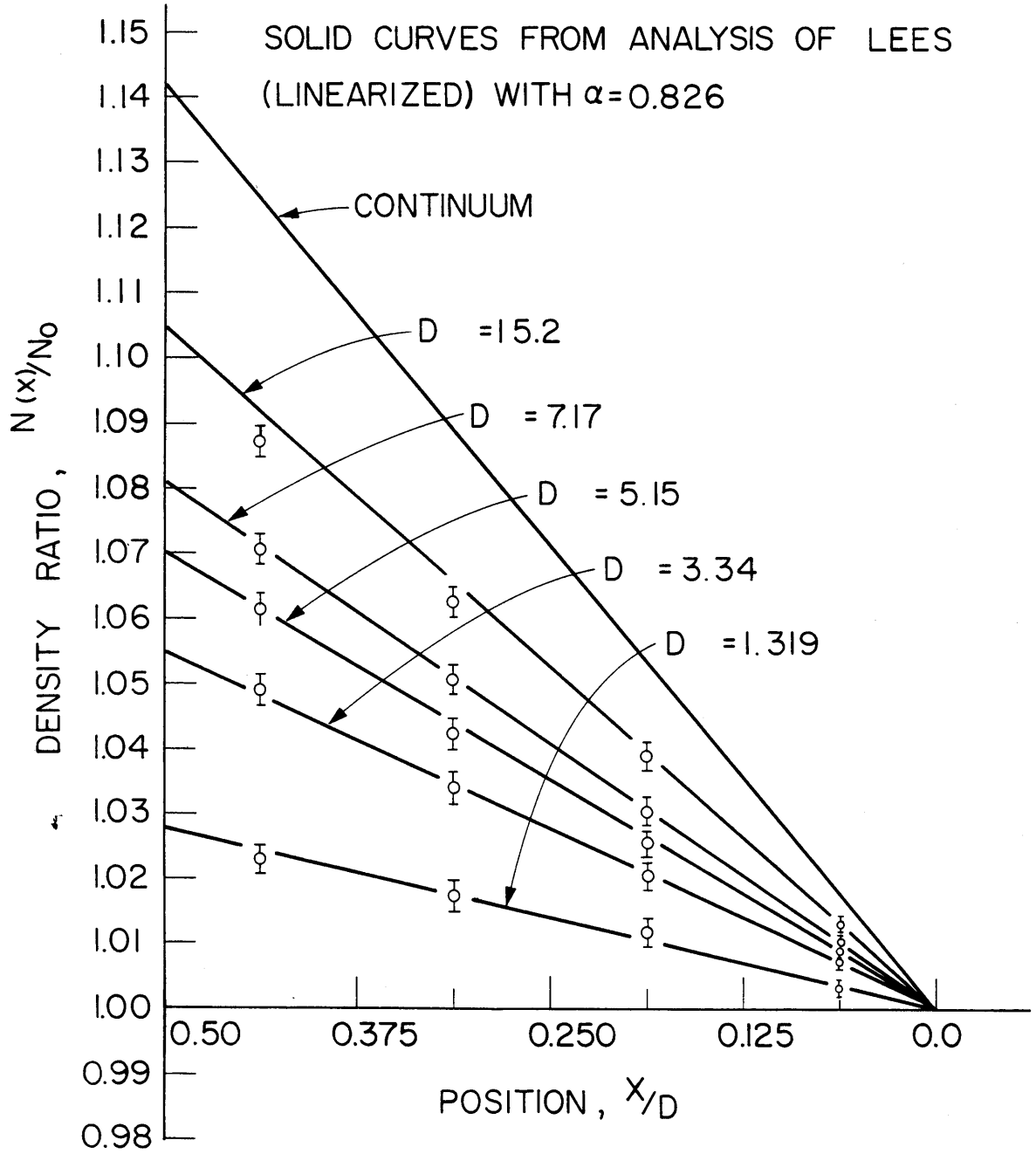

Fig. 5.2 Density Ratio Versus Position - Comparison Between Experimental Argon Results and the Results of Lees' Moment Method

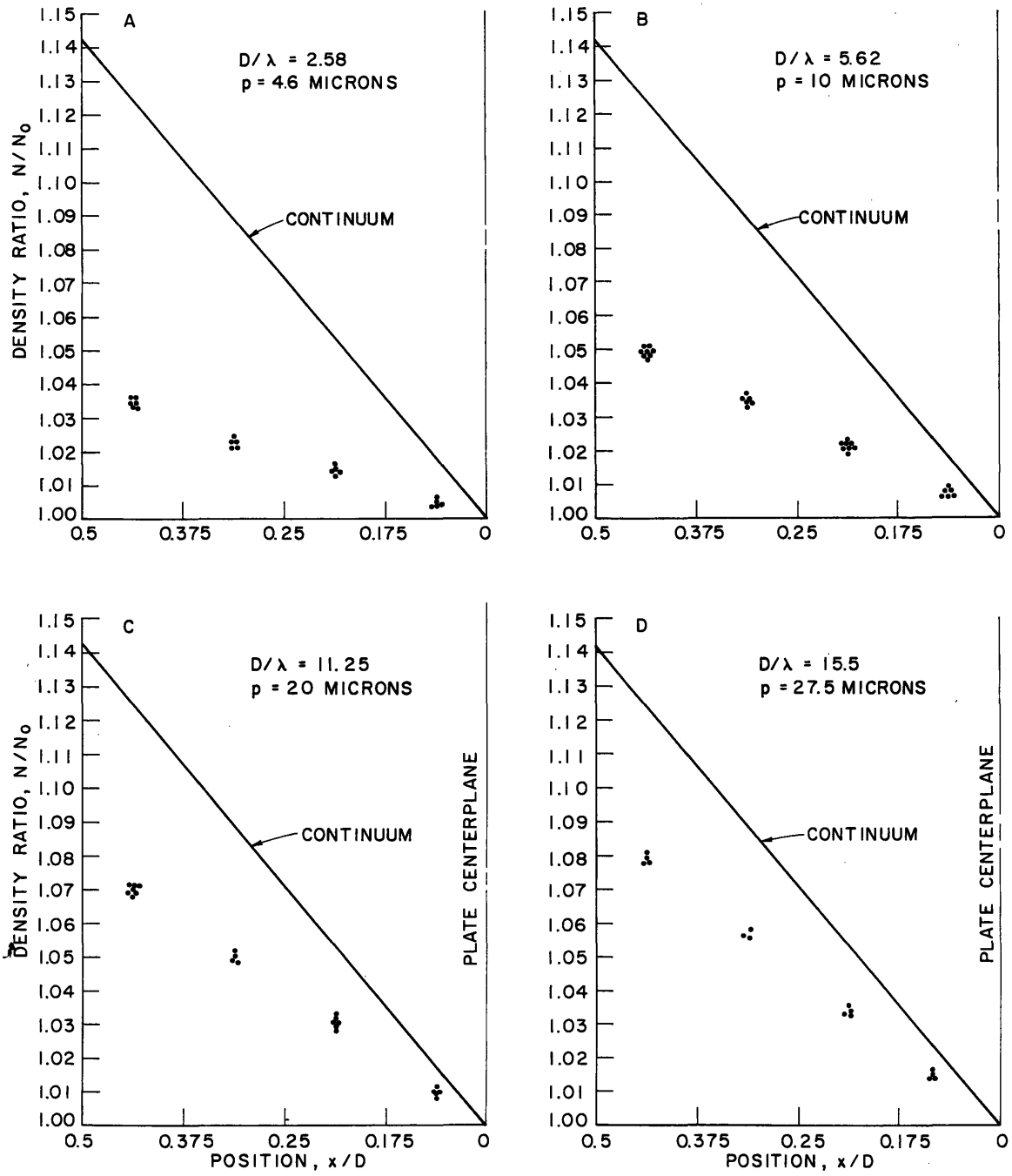

Fig. 5.3 Density Ratio Versus Position-
Nitrogen Experimental Results

Experimental Errors - Density Distribution:

The most probable causes of error and scatter in the density distribution measurements are:

(1) Poor optical alignment

(2) Incorrect pressure and temperature readings

(3) Unsteady electron beam current

(4) Non-linear relation between luminescence and density

These sources of error are discussed below:

Poor Optical Alignment:

The optical system was designed so that the portion of the beam luminescence measured was not a function of the position of the plates. To check if this was the case, readings were taken for various plate positions when the plates were at equal temperatures (i.e. constant density). The results indicated that the luminescence measured was independent of plate position until the beam approached closer than 1.59 mm away from either plate. The optical-photomultiplier system was, therefore, not a significant source of error so long as the beam did not approach closer than 1.59 mm from a plate.

Pressure and Temperature Readings:

As mentioned previously, the error in pressure readings for lower pressures was estimated to be ±3 pereent, and for higher pressure, ±1.5 percent. This error could lead to similar errors in the D/λ

values used in evaluating the density profiles from the analytical results.

The errors involved due to incorrect temperature readings were of negligible importance, since the temperature differences used for the density distribution measurements were about 1.50°F and it was possible to obtain this temperature difference to within 1/0°F.

Unsteady Beam Current and Reading Errors:

The scatter observed in the measured values of $N(x)/N_o$ (i.e. $I(x)/I_o$) is due to both fluctuations observed in the absolute luminescence level which are caused by an unsteadiness in the beam current and to the uncertainty inherent in reading this level on the Keithly meter. The scatter observed in the value of $(N(x)/N_o - 1)$ represents ±0.0025 units (see Figures 6.1 and 6.3) about an average value. The magnitude of this scatter is independent of the pressure level. The mean deviation of the measurements about an average value is about ±0.0014 units. This is assumed to be the probable error in any of the $(N(x)/N_o - 1)$ values due to scatter in the data.

Since this error due to scatter is independent of the pressure level, it results in a larger percentage error for the lowest pressure measurements where $(N(x)/N_o - 1)$ is smallest than for the higher pressure measurements where $(N(x)/N_o - 1)$ is largest. For example, ±0.0014 units represents an error of ±4.7 precent for the lowest pressure argon reading nearest the wall and ±1.1 percent for the corresponding highest pressure reading.

Non-Linear Relation Between Luminescence and Density:

There is the possibility that an error due to a non-linear relation between beam luminescence and density might be present for the highest pressure (32 micron) argon measurements. This possibility is indicated by one of the measurements being somewhat lower (5.5 percent) than would be expected if the four-moment results were valid. This is what one might expect if the relation between luminescence and density deviated slightly from being linear. Robbin and Talbot,[4] however, observed no such effect with argon for pressures less than 250 microns while using a blue filter before the photomultiplier. The source of this discrepancy is, therefore, not clear, but it is probably experimental. All the analyses which indicate any deviation from a linear density profile have it deviating in the opposite direction from that measured.

The above discussion indicates that the error in the density distribution measurements is expected to be mostly due to the scatter in the data.

The magnitude of the error in the value of $(\frac{N(x)}{N_o} - 1)$ due to scatter is estimated to vary from ±1.1 percent to ±4.7 percent for the argon measurements nearest the wall.

VII. DISCUSSION

The argon experimental results for both the heat transfer and the density distributions agree with the four-moment results of both Gross and Ziering, and Lees (linearized) and with the second approximation of Wang-Chang and Uhlenbeck for the complete range of inverse Knudsen numbers from free molecule to near continuum conditions. Also, the variation of these quantities with the accommodation coefficient is shown to be correctly described by these analyses, at least for values of ε near 0.8. Closest agreement between experiment and analysis is with those of Lees and Gross and Ziering where the average disagreement between the heat transfer measurements and the analytical results is about 2 percent and for the density distribution profiles about 3 percent. As indicated by the error bars on the experimental points, this casic agreement would be evident even if the maximum expected errors were present.

This agreement between experiment and the four-moment results is notable, inasmuch as theses analyses give final results for the heat transfer and density distribution in very simple analytical forms.

The four-moment results of Gross and Ziering and Lees do not indicate the presence of a Knudsen layer near the boundaries which results in the density profile deviating from being linear. Within the accuracy of this experiment, no such deviation from a linear density profile was measured. It should be noted, however, that a small deviation from a linear density profile could not be determined

by this experiment. The general agreement between the four-moment results and the experiment indicates, however, that an analysis which does not indicate a Knudsen layer can still be quite accurate in its description of such macroscopic quantities as the heat transfer and the density distribution. Conversely, an analysis which does indicate a Knudsen layer, does not necessarily accurately describe the heat transfer and density distribution as indicated by the lack of agreement between the experimental measurements and the eight-moment results.

NOMENCLATURE

Q	= actual heat conduction
Q_{FM}	= free molecule value of the heat conduction
$N(x)$	= density level of position, x
N_o	= plate centerplane density level
T_o	= plate centerplane temperature
$f(x,v)$	= velocity distribution function of a position, x
$f_M(T_o)$	= Maxwellian velocity distribution function of the plate centerplane conditions
ε	= "microscopic" accommodation coefficient
α	= thermal accommodation coefficient
λ	= mean free path of molecules
D	= Plate spacing
γ	= ratio of specific heats
C_v	= specific heat of constant volume
R	= gas constant
p	= pressure
KN	= Knudsen number = λ/D
I_b	= electron beam current
$I(x)$	= intensity of beam luminescence at a position, x
I_o	= intensity of the beam luminescence at the plate centerplane
v	= velocity of an individual molecule
v_x	= x component of the velocity
k	= thermal conductivity

REFERENCES

[1] C.S. Wang-Chang and G.E. Uhlenbeck, "Heat Transport Between Two Parallel Plates as a Function of Knudsen Number", University of Michigan Report M999, (1953).

[2] E.P. Gross and S. Ziering, "Heat Flow Between Parallel Plates", Phys. of Fluids, 2, p. 701, (1959).

[3] S. Ziering, "Shear and Heat Flow for Maxwellian Molecules", Phys. of Fluids, 3, p. 503, (1960).

[4] L. Lees and C.Y. Liu, "Kinetic Theory Description of Plane, Compressible Couette Flow", GALCIT Hypersonic Research Project, Memo NO. 58 (1960).

[5] M.L. Lavin and J.K. Haviland, "Application of a Momemt Method to Heat Transfer in Rarified Gases", Phys. of Fluids, 5, p. 274, (1962).

[6] J. K. Haviland and M. L. Lavin, "Application of the Monte Carlo Method to Heat Transfer in a Rarified Gas", Phys. of Fluids, 5, p. 1399, (1962).

[7] K. Frankowski, Z, Alterman, and C.L. Pekeris, "Heat Transport Between Parallel Plates in a Rarified Gas of Rigid Sphere Molecules", Phys. of Fluids, 8, p. 245, (1965).

[8] G.K. Bienkowski, "Kinetic Theory Analysis of Problems in the Transition Range of Knudsen Numbers", Ph.D. Thesis, Massachusetts Institute of Technology, Cambridge, Mass., (1962).

[9] M. S. Smoluchowski, "On Conduction of Heat by Rarified Gases", Phil. Mag. and Jour. Sci., 46, p. 192, (1898).

[10] J.K. Roberts, "The Exchange of Energy Between Gas Atoms and Solid Surfaces", Proc. Royal Society London, A129, 146 (1930).

[11] L.B. Thomas and R.C. Gohke, "A Comparative Study of Accommodation Coefficients by the Temperature Jump and Low Pressure Methods", J. of Chem. Phys., 22, 300, (1954).

[12] H.J. Bomelburg, "Heat Loss from Very Thin Heated Wires in Rarified Gases", Phys. of Fluids, 2, 717, (1959).

[13] K. Schafer, W. Arting, and A. Erken, Ann Physik (42) 176 (1942).

[14] N.V. Tsederberg, "Thermal Conductivity of Gases and Liquids", (The MIT Press, Cambridge, Massachusetts, 1965).

[15] H. Y. Wachman, "The Thermal Accommodation Coefficient: A Critical Survey", ARS. J., 32, 2, (1962).

[16] L. Lees, J. Soc. Indust. Appl. Math., 13, 278, (1965).

[17] P. Lasereff, "Uber den Temperatursprung an der Gienzc Zwischen Metall und Gas", Ann. Physik, 37, p. 233, (1912).

[18] W. Mandell and J. West, "On the Temperature Gradient in Gases at Various Pressures",

[19] A. Dybbs and G.S. Springer, "Experimental Study of Heat Conduction Through Rarified Gases Contained Between Concentric Cylinders", M.I.T. Fluid Mech. Lab. Report No. 65-2, (1965).

[20] M. Knudsen, Ann. Physik, 34, (1911).

[21] W.J. Taylor and H.L. Johnston, J. Chem. Physics., 14, 219 (1946).

[22] E.H. Kennard, Kinetic Theory of Gases, McGraw-Hill, New York, 1938.

[23] S. Dushman, Scientific Foundations of Vacuum Technique, J. Wiley, New York, 1949.

[24] E.P. Muntz, "Measurement of Rotational Temperature, Vibrational Temperature and Molecular Concentration in Non Radiating Flows of Low Density Nitrogen", VTIA Report 71 (1961).

[25] B.W. Schumacher and E.O. Gadamer, "Electron Beam Fluorescence Probe for Measuring the Local Gas Density in a Wide Field of Observation", Can. J. Physics, 36, p. 654, (1958).

[26] E.A. Gadamer, "Application of an Electron Gun to Density Measurements in a Rarified Gas Flow", VTIA Report 83, (1962).

[27] F. Robbin and L. Talbot, "Measurement of Shock Wave Thickness by the Electron Beam Fluorescence Method", Univ. of Cal. Report AS-65-4.

[28] S.L. Petrie, "An Electron Beam Device for Real Gas Flow Diagnostics", The Ohio State University, ARL Report 65-122, (1965).

[29] N. Cook and E. Rabinowicz, Physical Measurement and Analysis, Addison-Wesley, 1963.

APPENDIX I

LINEARIZATION OF THE LEES FOUR-MOMENT METHOD

The results obtained by Lees in Reference 4 are applicable for large as well as small temperatire differences between the plates. In this Appendix, a very brief outline is given on how these results are linearized by assuming a small temperature difference between the plates. Also, the boundary conditions are altered to allow for arbitrary values of the temperature accommodation coefficient.

The moment equations obtained by Lees on Page 14 of Reference 4 are:

$$\text{continuity:} \quad \bar{n}_1\bar{T}_1^{1/2} - \bar{n}_2\bar{T}_2^{1/2} = 0 \tag{1}$$

$$\text{momentum:} \quad \bar{n}_1\bar{T}_1 + \bar{n}_2\bar{T}_2 = C_1 \tag{2}$$

$$\text{energy:} \quad \bar{n}_1\bar{T}_1^{3/2} - \bar{n}_2\bar{T}_2^{3/2} = C_3 \tag{3}$$

$$\text{heat flux:} \quad d/d\bar{x}(\bar{n}_1\bar{T}_1^{2} + \bar{n}_2\bar{T}_2^{2}) + 4/15\,\frac{L}{\lambda_I}\,C_3(\bar{n}_1 + \bar{n}_2) = 0 \tag{4}$$

If the assumption is made that the temperature difference between the plates is small, so that:

$$\frac{T_{II}}{T_I} = 1 - \varepsilon \qquad \text{where:} \quad \varepsilon << 1$$

then:

$$\bar{n}_1 = 1 + N_1 \qquad \bar{T}_1 = 1 + t_1$$

$$\bar{n}_2 = 1 + N_2 \qquad \bar{T}_2 = 1 + t_2$$

where: $N_1, N_2, t_1, t_2 \ll 1$

The moment equations become:

$$N_1 + 1/2\ t_1 = N_2 + 1/2\ t_2 \tag{1'}$$

$$N_2 - N_1 = 1/2\ C_3 \tag{2'}$$

$$t_1 - t_2 = C_3$$

$$N_1 + t_1 = \text{const.} \tag{3'}$$

$$N_2 + t_2 = \text{const.}$$

$$d/d\bar{x}\ (t_1 + t_2) + 4/15\ L/\lambda_I\ C_2\ (2) = 0 \tag{4'}$$

Integrating 4' one obtains:

$$t_1 + t_2 = -\ 8/15\ L/\lambda_I\ C_3\bar{x} + C_4$$

Now, by taking into account the temperature accommodation at the plate defined by:

$$\alpha = \frac{T_r - T_i}{T_w - T_i} = \frac{\bar{T}_1 - \bar{T}_2}{1 - \bar{T}_2} \tag{5}$$

the following boundary conditions on t_1 and t_2 are obtained:

at $\bar{x} = 0$:

$$t_2 = -\ 1/\alpha_o\ C_3 \quad , \qquad t_1 = -\ C_3/\alpha_o(1 - \alpha_o)$$

$$N_1 = 0 \qquad\qquad N_2 = 1/2\ C_3$$

at $\bar{x} = 1$:

$$t_1 = 1/\alpha_L \ (C_3 - \alpha_L \varepsilon)$$

$$t_2 = 1/\alpha_L \ (C_3 - \alpha_L \varepsilon) - C_3$$

From equation 4' and the boundary conditions:

$$C_4 = C_3 - 2\ C_3/\alpha_o$$

and:
$$C_3 = \frac{\varepsilon}{1/\alpha_o + 1/\alpha_L - 1 + 4/15 - L/\lambda_1}$$

With C_3 evaluated in terms of ε, N_1, N_2, t_1 and t_2 can be evaluated and, therefore, the heat transfer and the density distribution between the plates can be determined.

Heat Transfer:

The ratio of the actual heat transfer to the continuum heat transfer is given by:

$$\frac{q}{q_\infty} = \frac{n_1 T_1^{3/2} \quad \frac{2k^3}{n\pi} \ C_3}{k_c \ T_i \ \varepsilon \ 1/L}$$

Substituting in the calculated value of C_3 and noting that for a monatomic gas that:

$$k_c = 15/4 \ \mu_1 \ k/m$$

$$\lambda_I = \frac{1}{3A_2\rho_1} \left(\frac{\pi\, kT_I}{K}\right)^{1/2}$$

$$\mu_1 = \frac{kT_I}{3/2\ A_2(2\ mk)^{1/2}}$$

this expression becomes:

$$\frac{q}{q_\infty} = \frac{1}{1 + (1/\alpha_o + 1/\alpha_L - 1)\ 15/4\ \lambda_1/L} \qquad (6)$$

Density Distribution:

The density distribution is defined by:

$$\langle n(x)\rangle = \int_{-\infty}^{\infty}\int_{-\infty}^{\infty}\int_{v_{x_o}}^{\infty} f_1(x,\bar{v})d\bar{v} + \int_{-\infty}^{\infty}\int_{-\infty}^{\infty}\int_{-\infty}^{o} f_2(x,\bar{v})d\bar{v}$$

where f_1 and f_2 are the assumed distributions found in reference 4 .

Carrying out the indicated integrations and linearizing:

$$\langle \bar{n}(x)\rangle = 1/2\ (n_1 + n_2) = 1 + \frac{N_1 + N_2}{2}$$

which, after a considerable amount of algebra, results in the expression:

$$\frac{n(x)}{n_o} = 1 + \frac{\bar{x}'}{1 + 15/4\ kN(2/\alpha - 1)}\ \frac{\Delta T}{T_o} \qquad (7)$$

where $\bar{x}'$ is the distance from the plate centerplane (note: $\bar{x}$ in the Lees analysis is the distance from the cold plate), ΔT is one half the temperature difference, and T_o is the plate centerplane temperature

assumed to be midway between the two plate temperatures. Also, in this expression the accommodation coefficient of the two plates were assumed equal.

Equations 6 and 7 are the equations used in evaluating the Lees linearized results.

APPENDIX II

EXTENSION OF THE LEES LINEARIZED RESULTS TO DESCRIBE THE HEAT TRANSFER RATIO FOR DIATOMIC GASES

The expression for the heat transfer ratio for monatomic gases as given by the Lees linearized results is:

$$\frac{Q}{Q_\infty}\Big|_m = \frac{1}{1 + 15/4\ \lambda/D\ (2/\alpha - 1)} \tag{1}$$

where Q_∞ is the continuum heat conduction. As suggested by Lees,[16] one might assume that the general expression for the heat transfer ratio to be of the form:

$$\frac{Q}{Q_\infty}\Big|_{general} = \frac{1}{1 + C\ \lambda/D(2/\alpha - 1)} \tag{2}$$

where C is a constant which depends on the type of molecule. A means of determining the value for C for diatomic molecules is presented in this section.

The expression for the free molecule heat conduction over the continuum heat conduction can be obtained from equation (1) by letting λ/D become large. For this case 1 becomes small relative to the term involving λ/D and, therefore:

$$\frac{Q_{FM}}{Q_\infty}\Big|_m = \frac{1}{15/4\ \lambda/D(2/\alpha - 1)} \tag{3}$$

For a monatomic gas, the free molecule heat conduction is proportional to $2R\Delta T$. For a diatomic gas there are, in addition to the three translational degrees of freedom, two rotation degrees of freedom which contribute to the energy transfer. The diatomic free molecule heat transfer is, therefore, proportional to $3R\Delta T$ (i.e. $2R\Delta T$ from the translational modes and $R\Delta T$ from the rotational modes). The diatomic free molecule heat conduction is, therefore, related to the monatomic heat conduction by:

$$Q_{FM}|_d = 3/2\ Q_{FM}|_m \tag{4}$$

It should be noted that this expression is valid only if the accommodation coefficients for the translational and internal modes of energy transfer are equal.

For a monatomic gas in the continuum limit, the heat conduction is proportional to $K\Delta T$, where K is the thermal conductivity. The value of K for a monatomic gas is given by Kennard[22] as:

$$K|_m = 5/2\ \mu C_v = 15/2\ \mu R \tag{5}$$

If Euler splitting of the internal modes of energy transfer is assumed, the diatomic value of the thermal conducticity is:[22]

$$K|_d = 5/2\ \mu(C_v)_T + \mu(C_v)_i = 17/2\ \mu R \tag{6}$$

In the continuum limit, therefore, the diatomic gas heat conduction is related to the monatomic heat conduction by:

$$Q_\infty|_d = \frac{17}{15}\ Q_\infty|_m \tag{7}$$

The following ratio can, therefore, be formed:

$$\frac{Q_{FM}}{Q_\infty}\Big|_d = \frac{45}{38} \frac{Q_{FM}}{Q_\infty}\Big|_m \tag{8}$$

Therefore:

$$\frac{Q_{FM}}{Q_\infty}\Big|_d = \frac{1}{3.166\ \lambda/D\ (2/\alpha - 1)} \tag{9}$$

The value of C for a diatomic gas is, therefore, seen to be 3.166.

The general expression for the heat transfer ratio is then:

$$\frac{Q}{Q_\infty}\Big|_d = \frac{1}{1 + 3.166\ \lambda/D(2/\alpha - 1)} \tag{10}$$

BIOGRAPHICAL NOTE

Mr. Teagan was born in Cambridge, Massachusetts, in 1939. After attending the Belmont, Massachusetts public school system, he attended Brown University where he received his B.Sc. in Engineering in 1961. In 1963 the author received his Sc.M. at M.I.T. in the Mechanical Engineering Department.

The author spent several summers gaining practical experience, working one summer at Dynatech Corporation in Cambridge, Mass. and another at the Naval Ordnance Laboratory in Silver Springs, Maryland. In addition, he taught engineering subjects for the academic year 1964-65 at New Haven College, in Connecticut.